Table 1
Development of amoebic abscess after hamster cheek pouch inoculation

Experiment	Inoculation	No. of animals inoculated*	No. of animals with abscess production (%)
1	*E. histolytica*	4	4 (100)
	E. dispar	4	0 (0)
2	*E. histolytica*	10	9 (90)
3	*E. histolytica*	4	3 (75)
4	*E. histolytica*	4	4 (100)
	Medium (TYI-S-33)	4	0 (100)

* Inoculum: trophozoites of *E. histolytica*, *E. dispar* 5×10^5/0.2 ml of TYI-S-33 media 0.2 ml of TYI-S-33, 15% BS media was inoculated as control.

pouches of all animals were inoculated with trophozoites of the *E. histolytica* SAW755 CR clone B study strain using a blunt esophageal tube placed inside of the cheek pouch without trauma to the tissue; Group 3—the backs of all animals inoculated intradermally with trophozoites of the *E. histolytica* strain SAW755CR clone B study strain using a tuberculin syringe

2.2.4. Experiment 4

Four male hamsters were used as sham controls in this study. Each animal was injected with *E. histolytica* trophozoites 5×10^5/0.2 ml of media in the right cheek pouch and with 0.2 ml of TY I-S-33 15% BS media in the left cheek pouch. All animals were examined for presence of amoebic abscess 5–7 days post infection.

2.3. Cheek pouch preparation

Methods were followed as described in detail by Handler and Shepro [5]. For animals given intradermal injections, each hamster cheek pouch was inoculated with *E. histolytica* trophozoites in a dose of 5×10^5 in 0.2 ml of medium. Injection was carefully performed using a tuberculin syringe until a bleb appeared. For each animal, amoebic abscesses were examined macroscopically for signs of inflammation or ulcer formation. Exudate from abscesses was aspirated with a pipette, a wet mount preparation was examined using a light microscope, and the presence of *E. histolytica* trophozoites was recorded. For killed animals, the cheek pouch was dissected, removed, and preserved in 10% formalin, and representative sections of specimens were submitted for histopathologic examination. After an overnight processing of dehydration and clearing, tissue blocks were embedded in paraffin, and 5 μ thick sections were cut from these blocks and stained using hematoxylin and eosin.

3. Results

Intradermal inoculation with axenically cultured trophozoites of the *E. histolytica* study strain readily and consistently produced infection in the cheek pouch of study animals; overall, 20 of 22 (91%) hamsters developed amoebic abscesses at the injection site (Table 1).

In experiment 1, animals inoculated with *E. histolytica* produced multiple cheek pouch lesions, whitish-yellow in color and with irregular borders (Fig. 1). Abscesses were semisolid with a thick brownish exudates that could be easily expressed; gram stain examination of this material demonstrated abundant polymorph nuclear leucocytes. In addition, live motile trophozoites were also seen. All animals were killed on day 7 by ether inhalation. The hamsters inoculated with *E. dispar* trophozoites showed no signs of active amoebic infection (Table 1).

In experiment 2, inoculation with trophozoites of *E. histolytica* produced abscesses as in experiment 1, in nine of 10 hamsters; one animal killed at day 2 post-inoculation did not show evidence of abscess formation. For the other serially killed hamsters, the largest abscesses and most visible

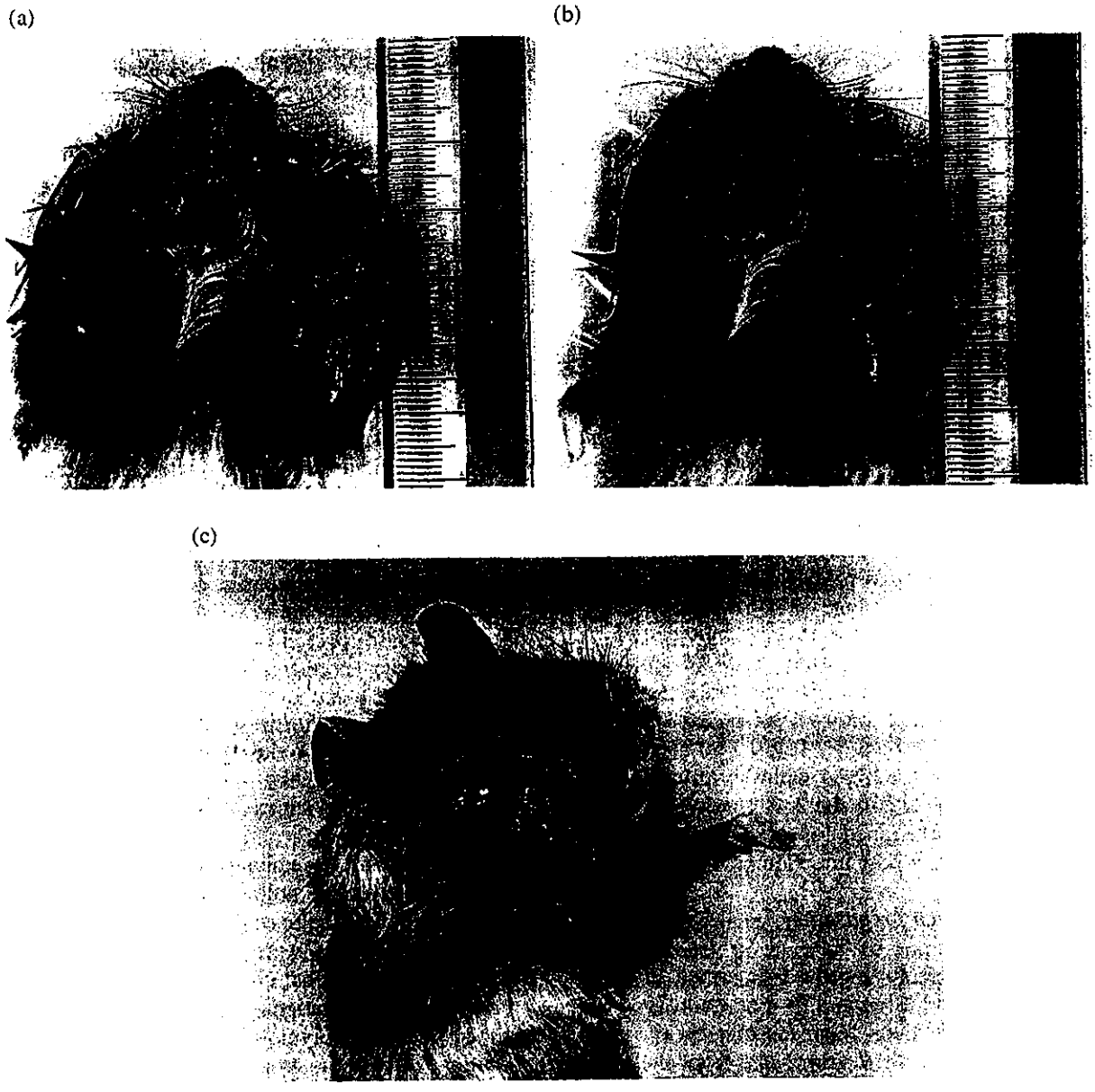

Fig. 1. Macroscopic abscesses of the hamster cheek pouch after intradermal injection of axenically grown *E. histolytica* trophozoites (a, day 7 with cheek pouch intact; b, day 7 with cheek pouch dissected away; c, day 12).

and motile trophozoites were seen on day 12 post-inoculation. At day 17, abscesses were smaller and no motile trophozoites were visible. Two animals died on day 20, at which time lesions had further resolved with residual scar tissue formation and no amoebic trophozoites seen on microscopy.

In experiment 3, hamsters injected with *E. histolytica* trophozoites into the cheek pouch demonstrated abscess formation. The abscesses produced in animals of group 1 showed maximal changes on day 12 post-inoculation, with motile trophozoites seen on light microscopy. One animal

from group 1 showed no infection and died 4 days post-inoculation. All remaining animals in-group 1 were killed at day 12. Animals inoculated with *E. histoloytica* without any tissue injury via blunt esophageal tube showed no signs of active amoebic infection. All four hamsters receiving back inoculation with *E. histolytica* developed abscesses; two animals were killed on day 7 and trophozoites were seen on histopathologic section. Two remaining animals were not killed to observe the natural history of infection: both died on days 14 and 19, respectively.

In experiment 4, all hamsters injected with *E. histolytica* trophozoites in the right cheek pouches produced abscesses but no abscess formation was observed in the left cheek pouches of hamster injected with TYI-S-33 media (Table 1).

3.1. Histopathologic findings

The cheek pouch mucous membrane was composed of a keratinized, stratified, squamous epithelium, which was supported by a thick layer of fibrous connective tissue. Three epithelial layers, spinosum, granulosum and corneum were apparent on light microscopic examination. The mucosa was further characterized by an absence of hair and glands. The lamina propria was composed of a fibrous connective tissue with many unusually large fat cells. This connective tissue was bordered by longitudinal skeletal muscle fibers. The pouch membrane was anchored to the subcutaneous connective tissue of the cheek by a layer of loosely packed areolar tissue. It was this region, which separated when the pouch was everted and injected with *E. histolytica* trophozoites, and led to abscess formation.

Histopathologic section from the cheek pouch abscess revealed granulation tissue only, the surface epithelium of the cheek pouch mucosa was completely ulcerated and no residual squamous epithelial cells were identified. The granulation tissue was composed of proliferating fibroblasts and new capillary-sized blood vessels separated by edematous and inflamed stroma.

The proliferating fibroblasts were spindle to polygonal in shape and had plump, oval, vesicular nuclei. The new capillary sized blood vessels were lined by cuboidal to flat endothelial cells. Some of the blood vessels were dilated and congested. Extravasation of erythrocytes into the stroma was also identified. The inflammatory cell infiltrate showed predominantly polymorphonuclear neutrophilic leucocytes and histiocytes along with lymphocytes and plasma cells. Foci of necrosis in the form of eosinophilic material and nuclear debris were present in the center of the abscess mixed with neutrophils. Numerous amoebic trophozoites with ingested erythrocytes were present in inflammatory exudates from these lesions (day 4, 7 and 12 post infection) and in tissue spaces (Fig. 2). No bacterial organisms were identified on the hematoxylin and eosin stained slides. Hamsters pouches from control animals, infected with *E. dispar* and TYI-S-33 media, respectively, showed

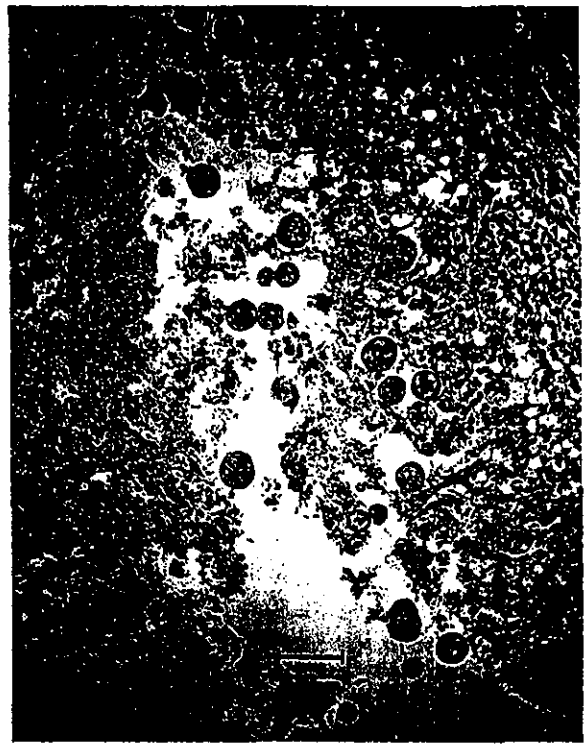

Fig. 2. Histopathologic sections of experimentally produced cheek pouch amoebic abscesses showing mixed inflammatory cell infiltration and numerous amoebic trophozoites with ingested red blood cells. (hematoxylin and eosin; 40× magnification).

normal stratified squamous epithelium with no evidence of any ulceration, acute inflammation or abscess formation. No amoebic trophozoites were seen.

Sections of the hamster back specimen also showed pathologic changes, which reflected abscess formation. The wall of the abscess was composed of granulation tissue showing proliferating fibroblasts, capillaries and oedematous stria infiltrated by mixed inflammatory cells. The center of the abscess revealed neutrophils, necrotic debris and amoebic trophozoites containing ingested erythrocytes.

4. Discussion

This preliminary study has shown that axenically-cultured *E. histolytica* trophozoites inoculated into the cheek pouch of hamsters can simply and reliably produce amoebic abscesses. The technique is highly efficient (91%) in establishing infection, and comparable to intraperitoneal or intrahepatic inoculation [4]. The procedure does not involve any major surgery, and it is less costly than other methods of inoculation. Intraportal or intrahepatic inoculation of trophozoites involves time-consuming procedures, which subsequently impose high risk to the animals from anesthesia and surgery.

The consistent development of the amoebic abscesses in this model may be attributed to the novel site of parasite implantation, ease of preparation and manipulation with minimum trauma to the tissues of the animal. The precise pathophysiologic mechanisms of disease have not been completely elucidated for invasive amoebiasis. The number of infecting trophozoites, volume of inoculum, and presence of virulence antigens all appear to be involved in abscess formation, but recent studies emphasize the role of the host immune-mediated process in the production of tissue necrosis and abscess formation, in response to immunogenic glycoproteins [21,22]. The results of Tsutsumi and colleagues, using intraportal inoculation of amebae, suggest that *E. histolytica* trophozoites do not produce liver abscesses through direct lysis of hepatocytes; rather, tissue destruction is the result of the accumulation and subsequent lysis of leukocytes and macrophages surrounding the parasites [23]. In particular, cell-mediated immunity and locally released cytokines such as tumor necrosis factor-alpha and interleukin-2 seem to play an important role in the pathogenesis of amoebic liver abscess formation [22,24,25]. Furthermore, our model supports the earlier observation by Gogler and Knight that antecedent trauma may facilitate the development of amoebic abscess formation [26]. The cheek pouches of 20 of 22 hamsters in our study inoculated intradermally with *E. histolytica* developed amoebic abscesses while; in contrast, invasive disease did not develop in any of the four animals inoculated by a traumatic blunt esophageal tube insertion. Amoebic trophozoites maintained axenically do not appear to require interaction with bacteria prior to tissue invasion.

We also injected animals with trophozoites of *E. dispar* and used sham controls injected with TYI-S-33 media. Both groups of animals showed no signs of infection and there were no pathologic changes. Furthermore, Gram stain of exudates from hamsters with amoebic abscess did not reveal any bacteria confirming the amoebic findings of histopathologic examination. Therefore, it seems unlikely that the inflammatory process was due to inadvertent bacterial contamination but we need to exclude the possibility that bacterial infection subsequent to inoculation may have contributed to the pathology we hope to investigate this in further studies.

The histopathological changes seen in our hamster pouch model correlate very well with the changes described for human intestinal amoebiasis disease by Prathap and Gilman [27] and Pittman and coworkers [28]. Initially non-specific inflammation and abscess formation were described with amoebae being only visible later with accompanying ulceration and necrosis. The difference between the architecture of the hamster pouch and hamster back abscess were subtle showing inflammation, abscess formation, granulation tissue and the presence of *E. histolytica* trophozoites. The hamster pouch abscess showed large areas of abscesses and necrosis with a proportionately fewer number of *E. histolytica* trophozoites. This may be in part due to the cheek pouch being an open space.

The amoebic abscess increased in size up to day 12-post inoculation and this correlated with the histopathologic findings. Abscesses resolved with healing although some animals died during the course of this study. In contrast, Ghadirian and Meerovitch [29] reported intrahepatic abscesses that resorbed after 17 days but animals showed clinical recovery and weight gain.

Our work has demonstrated the potential applications of this experimental model; however, further work is needed to elucidate the role of bacteria, *E. dispar* and virulent strains of *E. histolytica* in the pathogenesis of amoebic abscess.

In conclusion, this hamster cheek pouch model of amoebic abscess formation may help facilitate further study of the pathogenesis of invasive amoebiasis, and provide the opportunity to effectively examine therapeutic regimens in a controlled way. More sophisticated histopathologic and electron microscopic diagnostic techniques may help elucidate the evolution of early amoebic abscess lesions.

Acknowledgments

This work was financially supported by a visiting research fellowship from the Japanese Overseas Health Administration Centre and the Labor Welfare Corporation (Dr Beg). We would also like to express our sincere gratitude to Prof. T. Takeuchi, Department of Tropical Medicine and Parasitology, Keio University School of Medicine, Tokyo, Japan for permission to work in his laboratory. We also thank Prof. Viqar Zaman for his critical review of the manuscript and useful comments and appreciate the encouragement of Prof. Mushtaq Ahmed.

References

[1] Meerovitch E, Chadee K. In vivo models for pathogenicity in amebiasis. In: Ravdin JL, editor. Amebiasis: human infection by *Entamoeba histolytica*. New York: Wiley Medical, 1988. p. 177–90.

[2] Lushbaugh WB, Kairalla B, Hofbauer AF, Pittman FE. Sequential histopathology of cavitary liver abscess: formation induced by axenically grown *Entamoeba histolytica*. Arch Pathol Lab Med 1980;104:575–9.

[3] Mattern CFT, Keister DB. Experimental amebiasis. II: hepatic ameobiasis in the newborn hamster. Am J Trop Med Hyg 1977;26:402–11.

[4] Shibayama M, Campos-Rodriguez R, Ramirez-Rosales A, Flores-Romal A, Espinosa-Cantellano A, Martinez M, et al. *Entamoeba histolytica*: liver invasion and abscess production by intraperitoneal inoculation of trophozoites in hamsters, *Mesocricetus auratus*. Exp Parasitol 1988;88:20–7.

[5] Handler AH, Shepro D. Cheek pouch technique: uses and applications. In: Hoffman RA, et al, editor. The golden hamster: 'its biology and use in medical research'. Ames Iowa, USA: The Lowa State University Press, 1968. p. 195–201.

[6] Fulton GP. The golden hamster in biomedical research. In: Hoffman RA, et al, editor. The golden hamster: 'its biology and use in medical research'. Ames Iowa USA: The Iowa State University Press, 1968. p. 3–13.

[7] Delameter JN, Michaelson JB, Hallman FA, Blumenthal H. An investigation into hyaluronidase as a factor in the mechanism of tissue invasion by *Entamoeba histolytica*. Am J Trop Med 1954;3:1–8.

[8] Goodwin LG. Oedema in hamsters infected with Leishmania. Nature 1945;156:476–9.

[9] Goodwin LG. The chemotherapy of experimental leishmaniasis II: a dose response curve for the activity of sodium stibogluconate. Trans R Soc Trop Med Hyg 1945;39:133–45.

[10] Cram EB, Bozicevich J. Experimental *Schistosoma mansoni* infection by intraperitoneal injection. Trop Med News 1944;1:16–7.

[11] Stunkard HW. The Syrian hasmster, *Cricetus auratus*, host of *Hymenolepis nana*. J Parasitol 1945;31:151.

[12] Humes AG, Akers RP. Vascular changes in the cheek pouch of the golden hamster during the infection with *Trichinella spiralis* larvae. J Parasitol 1952;38:16–7.

[13] Boyd EM, Huston EJ. The distribution, longevity and sex ratio of *Trichinella spiralis* in hamsters following an initial infection. J Parasitol 1954;40:686–90.

[14] Bijovsky AT, Milder RV, Abrahamsohn IA, Sinhorini IL, Mariano M. The influence of lymphatic drainage in experimental *Trypanosoma cruzi* infection. Acta Trop 1984;41:207–14.

[15] Bijovsky AT, Milder RV. Ultrastructural analysis of the interactions between host cells and *Trypanosoma cruzi* in experimental chagomas. Trans R Soc Trop Med Hyg 1988;8:704–8.

[16] Franz DR, Lee M, Seng LT, Young GD, Baze WB, Lewis GE. Peripheral vascular pathophysiology of *Plasmodium berghei* infection: a comparative study in the cheek pouch and brain of the golden hamster. Am J Trop Med 1987;36:474–80.

[17] Nopdonrattakon L. Amoebiasis of the female genital tract: a case report. J Obstet Gyanaecol Res 1996;22:235–8.

[18] Purpon I, Jimenez D, Engelking RL. Amoebasis of the penis. J Virol 1967;98:372–4.

[19] Diamond LS, Harlow DR, Cunnick CC. A new medium for the axenic cultivation of *Entamoeba histolytica* and other *Entamoeba*. Trans R Soc Trop Med Hyg 1978;72:431–2.

[20] Kobayashi S, Imai E, Haghighi A, Tachibana H, Takeuchi T. Cultivation of *Entamoeba dispar*: growth-promoting effect of ferredoxin. Arch Med Res 2000;31:S210–S211.

[21] Rigothier MC, Khun H, Tavares P, Cardona A, Huerre M, Guillen A. Fate of *Entamoeba histolytica* during establishment of ameobic liver abscess analyzed by quantitative radioimaging and histology. Infect Immun 2002;70:3208–15.

[22] Seydel KB, Li E, Swanson PE, Stanley SL Jr. Human intestinal epithelial cells produce pro-inflammatory cytokines in response to infection in a SCID mouse-human intestinal xenograft model of amebiasis. Infect Immun 1997;65:1631–9.

[23] Tsutsumi V, Mena-Lopez R, Anaya-Velazquez F, Martinez-Palomo A. Cellular basis of experimental amebic liver abscess formation. Am J Pathol 1984;117:81–91.

[24] Agarwal SK, Khatri S, Anuradha S, Singh NP, Baveja U. Tumor necrosis factor-alpha and interleukin-1 in pus aspirate and blood in patients with amoebic liver abscess. J Assoc Physician India 1999;47:1065–7.

[25] Campbell D, Gaucher D, Chadee K. Serum from *Entamoeba histolytica*-infected gerbils selectively suppresses T cell proliferation by inhibiting interleukin-2 production. J Infect Dis 1999;179:1495–501.

[26] Gogler H, Knight R. The effect of hepatic injury upon the development of amoebic liver abscess in hamsters. Ann Trop Med Parasitol 1974;68:177–85.

[27] Prathap K, Gilman R. The histopathology of acute intestinal amoebiasis. Am J Pathol 1970;60:229–45.

[28] Pittman FE, El-Hashmi WK, Pittman JC. Studies of human amoebiasis II. Light and electron microscopic observations of colonic mucosa and exudates in acute amoebic colitis. Gastroenterol 1973;65:588–608.

[29] Ghadirian E, Meerovitch A. Behavior of axenic IP:106 strain of *Entamoeba histolytica* in the golden hamster. Am J Trop Med 1978;21:241–7.

Available online at www.sciencedirect.com

SCIENCE DIRECT

Parasitology International 54 (2005) 21–27

www.elsevier.com/locate/parint

Isolation and functional analysis of a *chk2* homologue from *Entamoeba histolytica*☆

Jun Iwashita[a,*], Yukita Sato[a], Seiki Kobayashi[b], Tsutomu Takeuchi[b], Tatsuya Abe[a]

[a]*Molecular Biology, Akita Prefectural University, Akita 010-0195, Japan*
[b]*Department of Tropical Medicine and Parasitology, Keio University School of Medicine, Tokyo 160-8582, Japan*

Received 22 March 2004; accepted 12 August 2004
Available online 1 October 2004

Abstract

Mammalian Chk2 is a Ser/Thr kinase required for cell-division arrest induced by DNA damage. We found six new kinase genes of *Entamoeba histolytica* by analysis in silico. One of the kinase genes was a homologue of human *chk2* gene. The *chk2* homologue gene (*Eh chk2*) was expected to encode 398 amino acids and showed nearly 50% homology to human Chk2 in amino acid sequence. *Eh chk2* had a catalytic domain of Ser/Thr kinase and a fork head-associated (FHA) domain that is highly conserved among Chk2 homologues in vertebrates. To examine the biological functions of *Eh chk2*, we synthesized *Eh chk2* mRNA in vitro and injected it into immature frog eggs (*Xenopus laevis* oocytes) as a model system of cell division. *Eh chk2* markedly delayed the cell division of frog eggs by disrupting transition of G2 phase to M phase. *Eh chk2* also inhibited the activation of p42 MAPK and Cdc2 kinase which are representative events induced by cell division. These results suggest that *Eh chk2* gene should be a cell-division regulator in *E. histolytica*.
© 2004 Elsevier Ireland Ltd. All rights reserved.

Keywords: *Entamoeba histolytica*; Chk2; Kinase; Cell division

1. Introduction

Entamoeba histolytica, an enteric protozoan parasite, is the cause of human amebiasis [1–3]. Amoebic trophozoites of *E. histolytica* proliferate in the human colon or liver and often cause tissue destruction. Although proliferation of trophozoites is an important factor in amoebic diseases, regulation of cell division is not fully understood at the molecular levels.

The regulation of cell division is studied well in eukaryotic cells. In eukaryotes, a cell cycle is separated into two major phases, the resting interphase and mitotic M phase. Once interphase cells enter in M phase, they start dividing irreversibly. The key regulator of cell division is a complex of two proteins, CyclinB and Cdc2. Cdc2 is a member of cyclin-dependent protein kinases (Cdks). The activity of Cdc2/CyclinB complex is inhibited in interphase. Once Cdc2/CyclinB is activated, the cells enter M phase and start dividing [4–8]. The activity of Cdc2/CyclinB is directly regulated by Cdc25 phosphatase. Cdc25 phosphatase dephosphorylates Tyr-15 of Cdc2 and activates it for progression into M-phase [9]. When DNA is damaged or replicated defectively, the cell cycle is arrested at a checkpoint in the interphase by inhibiting the activity of Cdc25 phosphatase. In arrested cells, Cdc25 is phosphorylated at Ser-216 by Chk1 or Chk2 kinase (a homologue of yeast Cds1) to lose its activity [10]. Chk2 is an important kinase which inhibits cell cycle at checkpoints, especially in DNA damage at S phase or G2 phase. The activity of mammalian homologue of Chk2 appears to require a checkpoint protein kinase, Ataxia telangiectasia mutated (ATM), which phosphorylates and activates Chk2 [11–13].

In *E. histolytica*, some cell-cycle regulating genes, *Eh cdc2*, *ras*, *rap*, *mfk1* and *rho* homologue, have been isolated [14–18], however, with the exception of *Eh cdc2*, these

☆ Nucleotide sequences data reported in this paper are available in the GenBank data base under the accession numbers: AB118100 (Eh1119), AB118101 (Eh1751), AB118102 (Eh1826), AB118103 (Eh2109), AB118104 (Eh6121), AB118573 (*Eh S6*) and AB118105 (*Eh chk2*).

* Corresponding author. Tel.: +81 18 872 1570; fax: +81 18 872 1676.
E-mail address: jun_iwashita@akita-pu.ac.jp (J. Iwashita).

1383-5769/$ - see front matter © 2004 Elsevier Ireland Ltd. All rights reserved.
doi:10.1016/j.parint.2004.08.002

genes are no central regulator genes that directly control the activity of Cyclin–Cdk complex. We isolated a homologue of S6 kinase (*Eh S6*) from *E. histolytica* cDNA library (accession No: AB118573). In this study, using the information of amino acid sequences of *Eh S6*, we found other six new kinase genes of *E. histolytica* including a homologue of human *chk2* (*Eh chk2*) by analysis in silico. The isolated *Eh chk2* gene had a fork head-associated (FHA) region which is characteristic of human *Chk2*. *Eh chk2* mRNA transcribed in vitro could induce a delay of cell division in immature frog eggs. *Eh chk2* gene should be a cell-division regulator in *E. histolytica*.

2. Materials and methods

2.1. Preparation of genomic DNA and Polymerase chain reaction (PCR)

E. histolytica strain HM1:IMSS was cultured in TYI-S-33 medium axenicly at 35.5 °C in vitro [19]. Genomic DNA was prepared from *E. histolytica* trophozoites (10^8) with a standard method [18]. We searched new kinase genes with *Eh S6* sequence in the *E. histolytica* genome database of the institute for genomic research (TIGR; http://www.tigr.org/tdb/e2k1/eha1/). TIGR database informs that preliminary sequence data for *E. histolytica* is deposited regularly into the GSS division of GenBank. We performed PCR to amplify cDNA fragments of kinases that were found by the DNA homology search in TIGR database. The PCR was 30 cycles of 90 °C for 1 min, 50 °C for 1 min and 72 °C for 2 min with 0.1 μg of the genomic DNA and primers described below. The PCR products were detected by electrophoresis on a 1.5% agarose gel containing ethidium bromide. PCR primers used are as follows:

Eh1119 forward primer: 5′-GAACTCGAGACCATGA-GAAGAACTTTTCAGTT-3′
Eh1119 reverse primer: 5′-CCTCTAGATAAA-CACTTCTTCGGATAGTTCA-3′
Eh1751 forward primer: 5′-TTTCTCGAGACCAT-GAGTGATGGAAATGAAAT-3′
Eh1751 reverse primer: 5′-TTTTCTAGACAAACT-CAGTTCATATTTAAAAT-3′
Eh1826 forward primer: 5′-AAACTCGAGACCATGT-CAAGTGAAACTCCAAC-3′
Eh1826 reverse primer: 5′-AAGTCTAGACTTTAACC-CATTGTCTTTCCTTG-3′
Eh2109 forward primer: 5′-AGTCTCGAGACCATGT-CAAAGGAAGTTGGAGA-3′
Eh2109 reverse primer: 5′-AAGTCTAGAAAATAT-CAAAAATAAAAACAAAC-3′
Eh6121 forward primer: 5′-CAACTCGAGACCAT-GAAAATATTAAATAAAAC-3′
Eh6121 reverse primer: 5′-AAATCTAGAGGTTGT-TATTTACCCACATATGT-3′
Eh chk2 forward primer: 5′-TAACTCGAGAC-CATGTGGGGAAAATTTGTTTG-3′
Eh chk2 reverse primer: 5′-GACTCTAGAAATTA-GACTTAAATAATATCTTT-3′
β-actin forward primer: 5′-CGCCTCGAGACCATG-GATGATGATATCGCCGC-3′
β-actin reverse primer: 5′-GCCATCCTGCGTCTG-GACCT-3′

All primer sets contain a kozak sequence [20] and *Xho*I site in their forward primers and *Xba*I site in their reverse primers.

2.2. DNA sequence analysis

DNA sequences were determined with a BigDye Terminator Cycle Sequencing Ready Reaction Kit (Applied Biosystems, Tokyo, Japan) using an ABI 310 DNA sequencer (Perkin Elmer, CT, USA). Sample mixtures (10 μl), which contained 10 ng of cDNA, 1.6 pmol of forward and reverse PCR primers and 4 μl of the kit reagent, were reacted for sequencing PCR. The PCR was 25 cycles of 96 °C for 30 s, 50 °C for 15 s and 60 °C for 4 min.

2.3. Construction of recombinant plasmids and in vitro mRNA transcription

Six new kinase genes, which have an entire open reading frame, were amplified by PCR with primers designed for cutting out. After appropriate PCR, PCR products of the kinase genes were digested with restriction enzymes, *Xba*I and *Xho*I, and subcloned into pT7G vector. The amplified pT7G recombinant plasmids were digested with only *Xho*I and then transcribed in vitro with T7 RNA polymerase using a MEGAscript T7 kit (Ambion, Austin, USA) to obtain 5′ - capped mRNAs.

2.4. Detection of functions of kinase mRNA in Xenopus eggs

Eggs were collected from an ovary of *Xenopus laevis*. Stage VI immature eggs were defolliculated by treatment with 1.5 mg/ml of collagenase (Wako, Osaka, Japan). One shot of 60 nl of 0.2 mg/ml of mRNA, which was transcribed in vitro and solubilized in RNase-free water, was injected into about 20 eggs. The mRNA-injected eggs were exposed to 1 ng/ml of progesterone hormone (Wako) after 12 h of injection and cultured in modified Barth's solution at 23 °C [21,22]. Entry into M-phase was estimated by the germinal vesicle breakdown (GVBD), which accompanied a small white spot on the animal pole of eggs. Percentage of white spotted eggs was obtained by several intervals.

2.5. Western blot analysis

The treated eggs were dissolved in Laemmli's sample buffer [23] and heated at 98 °C for 3 min. And then, those

samples were applied to 12% SDS-polyacrylamide gel. Proteins on the gel were transferred to a nitrocellulose membrane (Hybond ECL: Amersham Pharmacia Biotech, USA) using a transfer apparatus (Cima Biotech, MN, USA). After transfer, the membrane was incubated with a blocking buffer of 20 mM Tris–HCl, 150 mM NaCl and 0.1% Tween-20, pH 7.5 (TBS-T) containing 4% skimmed milk (Gibco Oriental, Tokyo, Japan) at room temperature for 1 h. The membrane was incubated with anti-Cdc2 monoclonal antibody (1:5000; PSTAIR, Santa Cruz Biotechnology, USA), anti-phospho-p44/p42 MAP kinase (Thr-202/Tyr-204) E10 monoclonal antibody (1:5000; Cell Signaling Technology, MA, USA), or anti-ERK 1/2 polyclonal antibody (1:5000; Promega, WI, USA) in the blocking buffer at room temperature for 1 h. After washing with TBS-T, the membrane was incubated for 1 h with goat anti-rabbit IgG (H+L) antibody conjugated with horseradish peroxidase (1:5000; Promega) for Cdc2 detection, or with goat anti-mouse IgG antibody conjugated with horseradish peroxidase (1:5000; Promega) for p42 MAPK detection. Enzyme reaction was detected with enhanced chemiluminescence by an ECL kit (Amersham Pharmacia Biotech, Buckingham-

```
Ehchk2      1  ----------------------------------------------MWGKFVCEQFHKEIP
human       1  ------------------------------------------------------RD*SCE
drosophila  1  --------------MARDTQGTQGTQSQASNIWTQVESQPMEKIVWGRLYGKNIKI*SLD
elegans     1  MVRGTKRRRSSAEKPIVVVPVTRDDTMPVDEDLVVGESQCAASKPFAKLVGVRRGISS*D
rad53       1  -----------MENITQPTQQSTQATQRFLIEKFSQEQIGENIVCRVICTTGQIPIRDLS

Ehchk2     16  FNKGEMIIGR----------KAYEFLSSIVKVSVIHCIIKRSELPNLTVTTITDKSTNGT
human       7  YCFD*PLLK*-------------TDKYRTYSKKHFRIFREVG-PK*SYIAY*E*H*G***
drosophila 47  L*ND*FTA**GEANDLILTLNDLPEKILTRISK*HFI*KRAN-CELTNPVY*Q*L*R***
elegans    61  LADDHFVC**GSDDAPTNFNFSQVAKDVGLYRFISKIQFSIDRDTETRRIYLH*H*R***
rad53      50  ADISQVLKEKRSIKKVWTFGRNPACDYHLGNI*RLSNKHFQIL*GEDGNLLLN*I*****

Ehchk2     66  YLNGERLEKNLETYLSCFDEITFLNKITQPDYITFDYYDSTIIDLINKQCS---------
human      53  FV*T*LVG*GKRRP*NNNS**ALSLSRNKVFVFFDLTV*DQSVYPKALR----------
drosophila 106 FV*N*KIGT*RMRI*KND*V*SLSHPTYKAFVFKDLSPNES*GLPEEIN----------
elegans    121 LV*Q*MIG*G*SRE*MNG*L*SIGIPALIIFVYESADA*HHP--EELTK----------
rad53      110 W***QKV***SNQL**QG****VGVGVESDILSLVIFINDKFKQCLEQNKVDRIRSNLKN

Ehchk2     116 ------------------------LFKKYQLGKYIGKGSFGVVREIMELATNTKFAIKII
human      101 -------------------------DE*IMS*TL*S*AC*E*KLAF*RK*CK*V*****
drosophila 154 -------------------------*T*YVNRKL*S*AY*L**LVYDTR*CQQ**M**V
elegans    167 -------------------------*YHVTSHSL***G**K*LLGYKKSDRSVV***QL
rad53      170 TSKIASPGLTSSTASSMVANKTGIFKDFSIIDEVV*Q*A*AT*KKAI*RT*GKT**V***

Ehchk2     153 NKE---------KAKNSLNQIHRECNTMKKINHPNSVKFKELFETNEMIFVIMELINGTT
human      136 S*RKFAIG--SAREADPALNVET*IEIL**L***CII*I*NF*DAED-YYIVL**ME*GE
drosophila 189 K*NMLSGARPSTNFSDPDR-VLN*AKI**NLS**CV*RMHDIVDKPDSVYMVL*FMR*GD
elegans    202 *---TQFSTRCSR*IAKTRD*RN*VEV***LS***I*AIYDWITVAKYSYMVI*YVG*GE
rad53      230 S*R---------*VIGNMDGVT**LEVLQ*L***RI*RL*GFY*DT*SYYMV**FVS*GD

Ehchk2     204 LEKVLKENSLS-----HQEKNDIIIELLQLLKYLHSIDIVHRDIKPENLMITRIKDEIHI
human      193 *FDKVVG*KR----LKEATCKLYFYQM*LAVQ***ENG*I***L****VLLSSQEEDCL*
drosophila 248 *LNRIIS*K*----LSEDISKLYFYQMCHAV****DRG*T***L**D*VLLETNDE*TLL
elegans    259 FFSKVVDSKYNRMGLGESLGKYFAFQ*IDAIL****VG*C********ILCSDKAERCIL
rad53      281 *MDFVAAHGAVG----EDAGRE*SRQI*TAI**I**MG*S***L**D*IL*E-QD*PVLV

Ehchk2     259 KLIDFGFGKELTGTIHAATLCGTPLYAAPELFEDKKTG----------YDARKIDIWSAG
human      249 *IT***HS*I*GE*SLMR******T*L***VLVSVG*----------AGYN*AV*C**L*
drosophila 304 *VS***LS*FVQKDSIMR********V***VLITGGR----------EAYTK*V****L*
elegans    319 **T***MA*NSVN--RMK*R****S*N***IVANEG----------VEYTP*V****L*
rad53      336 *IT***LA*VQGNGSFMK*F***LA*V***VIRG*D*SVSPDEYEERNEYSSLV*M**M*

Ehchk2     309 VIIYIILTGRHPFCSNDYKIKELLDNIQHNSYSSFPCFNLLTDSQQLLLKGMFDSDVSKR
human      299 **LF*C*S*YP**SEHRTQVSLKDQITSGKYNFIPEVWAEVSEKALD*V*KLLVV*PKA*
drosophila 354 *VLFTC*S*TL**SDEYGTP-AAQQIKKGRFAYGH*SWKSVSQRAK**INQ*LIV*PER*
elegans    366 CVLF*TFS*YP**SEEYTDMTMDEQVLTG-RLIFHAQWRRI*VET*NMI*W*LTVEP*N*
rad53      396 CLV*V****HL**SGS-TQDQLYKQIGRGSYHEGPLKDFRISEEARDFIDSLLQV*PNN*

Ehchk2     369 FSASECLECLQRKRQKEISDVFCSSKKDII----------------------------
human      359 *TTE*A*RHPWLQDEDMKRKFQDLLSEENESTAL----------------------------
drosophila 413 P*IDDV*QSSWLGDAPMLQKAKRLM*L*GMEIEE----------------------------
elegans    425 P**V*LMSTQWM*CADCRTAKQDIL*SIKPISAA----------------------------
rad53      455 ST*AKA*NHPWI*MSPLG*QSYGDFSQISLSQSLSQQKLLENMDDAQYEFVKAQRKLQME
```

Fig. 1. Comparison of chk2 ORF between *Eh chk2*, human, Drosophila, *C. elegans* and *S. cerevisiae*. The names of databases and accession numbers of the homologues are as follows; human chk2 (GenBank, AF086904), Drosophila chk2 (GenBank, U87984), *C. elegans* chk2 (SWISS-PROT, CHK2_CAEEL), *S. cerevisiae* CHK2/RAD53 (PIR, A39616) Asterisk marks the identical amino acid residues. A FHA homology region is underlined. Highly conserved amino acid residues of FHA domain are bolded.

shire, UK) and an image analyzer LAS-1000 plus (Fujifilm, Tokyo, Japan).

3. Results

3.1. Cloning of a chk2 homologue of E. histolytica

Cell cycle is regulated by the interplay of many molecules, such as Cdks, Cyclins, and cell-cycle checkpoint kinases. Among those molecules, Ser/Thr kinases are the most important regulators. We isolated a S6 kinase of *E. histolytica* (*Eh S6*: AB118573). In order to look for new cell-division regulator genes of *E. histolytica*, we used TIGR *E. histolytica* genome database, which is an open database containing *E. histolytica* genome sequences. We performed a homology search in the *E. histolytica* genome database using a DNA sequence of conserved Ser/Thr kinase catalytic domain of the *Eh S6* gene. As a result, we found six new *E. histolytica* kinase genes that contain an entire open reading frame and a catalytic domain sequence of Ser/Thr kinase (Figs. 1 and 2) (Table 1). One of the newly assigned genes had 52% homology in overlapping region to the human *chk2* gene in amino acid sequence and designated *Eh chk2* (Fig. 1). The DNA sequence of *Eh chk2* contained about 1.2 kbp of no intron region within it.

```
A)
Eh1119      61  DKASICSRPEKKRKVERELAILRIIHHPNIIDYYASYETTKLLFVVQELLSGGELYTYVE
humansnf    59  **TRLD*--SNLE*IY**VQLMKLLN**H**KL*QVM**KDM*YI*T*FAKN**MFD*LT
Gthetasnf   47  K*DLFYDK*SLRL*IQ**ISVMKLMF**HV*KI*DVL*DS*Y**LII*YA*K***FN*LV

Eh1119     121 KKKKLSLEESVKFLLQILSALKYIHKWQICHRDVKLENILLSHDCSTAKLCDFGMATYTG
humansnf   117 SNGH**EN*AR*KFW*****VE*C*DHH*V***L*T**L**DGNMDIKLADFGFGNF*KS
Gthetasnf  107 E*R**ENR*AL**FHE*I*G*E*C**HR*****L*******DMKLQIKIADFGMASLSIP

Eh1119     181 GMPLRDSCGSPFYAAPELFTQPTYDGCIADIWSLGVVFYVMIFGLMPFP--GETDEEFVE
humansnf   177 *E**STW****P*****V*EGKE*E*PQL********L**LVC*SL**D--*PNLPTLRQ
Gthetasnf  167 NIM*KTF****H**S**VVSNEP*N*IK*****C*IIL*ALVV*KL*YDEENDNMRKLFN

B)
Eh1751     276 VVVIQMEYCSGSNLSRIIESQELHYSKKNANEKINFYFKQIITGIQYIHSKNIIHGDLKP
humanTIK   361 CLF****F*DKGT*EQW**KR---RGE*LDKVLALEL*E**TK*VD*****KL**R****
mouseTIK   323 CLF****F*DKGT*EQWMRNR---NQS*VDKAL*LDLYE**V**VE*****GL**R****

Eh1751     336 ANIFR-DGDILKIGDFGYATMAKNRNK--CKFVGTPGYTAP-EVSSGDYDTSIDIYSLGI
humanTIK   418 S***LV*TKQV******LV*SL**DG*-RTRSK**LR*MS*EQI**Q**GKEV*L*A**L
mouseTIK   380 G***LV*ERHI******L**ALE*DG*SRTRRT**LQ*MS*EQLFLKH*GKEV**FA**L

Eh1751     392 ILLEMCMSCVTRSEFILGIELIKKR----------------QINETVSKYFPQLSQLILN
humanTIK   477 **A*LLHV*D*AF*TSKFFTDLRDG-IISDIFDKKEKTLLQKLLSKKPEDR*NT*EILRT
mouseTIK   440 **A*LLHT*F*E**K*KFF*SLR*GDFSNDIFDNKEKSLLKKLLSEKP*DR*ET*EILKT

C)
Eh1826     203  PEDQLEMIKREIQLMRQLHHKNIVKLFDVYENNE-ILYLILEYVEGGELYDRLVQGALN-
Eh2109      45  DP---QKLQG**KILKMVD*PY*I**Y**FDG*DGK**I*TDL*K****F**ISDKTFYP
humanMLK  1501 K*K--*N*RQ**SI*NC***PKL*QCV*AF*EKA-NIVMV**I*S****FE*IIDEDFEL

Eh1826     260  -ERQAACVLYQLVSAITYLHKNNIAHRDLKPENILCVYKN-KLYIKIADFGLSKDFST--
Eh2109     101  -*DK*KI*VKR*I***G***SM**V**********LKSPDDDTDVR*****F**MITEDA
humanMLK  1558 T**ECIKYMR*ISEGVE*I**QG*V*L*******M**N*T-GTR**LI****ARRLEN-A

Eh1826     317  SLLQTCCGTPSYVAPEIIKGDCYTCQCDIWSIGVITYLVLSGNLPFYDENEEVIFDKILD
Eh2109     161  QI*L*A****V*****VLNAKG*GMEV*M********VL*C*YP**FGDTLGE*LSAVCA
humanMLK  1616 GS*KVLF***EF****V*NYEPIGYAT*M******C*ILV**LS**MGD*DNETLANVTS

D)
Eh6121      66  HRFSIERTRFYAAELLIGLKYLHDAGIVYRDLKPENILLTDEGHVCITDFGLCKEG-LTE
DdisRac    213 KK*TED*V*Y*G**IVLA*EH**LS*VI********L***N***I*M*********L**P
humanRac   241 RV**ED*****G**IVSA*D***SGK*******L**LM*DKD**IK**********-I*D

Eh6121     125 KDQTNTFCGTPEYLAPEILLGNGYGFAVDWWSYGTLIYEMLLGLPPFFDNDVQTMYQKIV
DdisRac    273 T*K*G***********V*Q*****KQ*****F*S*L****T*****YNQ***E**R**M
humanRac   300 AATMK***********V*ED*D**R*****GL*VVM***MC*RL**YNQ*HEKLFEL*L

Eh6121     185 SDDVRFPKNTPPAIREFISALLQKDPEDRLT----NPDIMXKHPFFKNMDFEMVKAKKIK
DdisRac    333 MEKLS**HFIS*DA*SLLEQ**ER***K**A----D*NLIKR****RSI*W*QLFQ*N*P
humanRac   360 ME*IK**RTLSSDAKSLL*G**I***NK**GGGPDDAKEIMR*S**SGVNWQD*YD**LV
```

Fig. 2. Comparison of overlapping region of newly cloned *Eh* kinases and homologues. (A) Eh1119, human snf1 (GenBank, BC038504) and *Guillardia theta* snf1 (PIR, B90120). (B) Eh1751, human TIK (GenBank, U50648) and mouse TIK (PRF, 1715268A). (C) Eh1826, Eh2109 and human MLK (GenBank, AY339601). (D) Eh6121, *Dictyostelium discoideum* Rac (SWISS-PROT, KRAC_DICDI) and human Rac (SWISS-PROT, AKT3_HUMAN). Asterisk marks the identical amino acid residues.

Table 1
Newly cloned *Eh* kinases

Clone name	Length (bp)	Accession number	Segment number of TIGR	Homologue
Eh1119	1797	AB118100	316759	SNF1
Eh1751	1311	AB118101	317284	PKR(TIK)
Eh1826	1371	AB118102	318129	myosin L chain kinase
Eh2109	810	AB118103	316894	myosin L chain kinase
Eh6121	1398	AB118104	318097	Rac1
Eh chk2	1194	AB118105	317604	Chk2

The nucleotide sequence data reported in this paper appear in the DDBJ, EMBL and GenBank nucleotide sequence databases with the accession numbers as indicated. Reference segment numbers of TIGR database are shown. Homologues were deduced by the expected amino acid sequences.

Expected amino acid sequence of *Eh chk2* contained a FHA domain in its N-terminal region (Fig. 1) which is conserved region in eukaryotic Chk2 [24,25]. Amino acid sequences of FHA domain have diversity with 55–75 residues, but seven amino acid residues are highly conserved among eukaryotic FHA domains [26]. All of those conserved seven amino acid residues were found in the putative FHA domain of *Eh chk2* (Fig. 1).

3.2. Functions of Eh chk2 in vivo

Human Chk2 kinase is a critical inhibitor of cell division. We tried to ensure the in vivo function of *Eh Chk2* in cell-division regulation. For functional analysis, we used immature eggs of the amphibian, *Xenopus laevis*, which is a common system for cell-cycle analysis. The immature *Xenopus* egg is naturally arrested at G2 phase with low activities of p42 MAP kinase and Cdc2/CyclinB complex. Progesterone hormone stimulates the activities of MAP kinase and Cdc2/CyclinB complex, and makes egg enters cell division. This event accompanies chromosome condensation and nuclear envelope disruption (GVBD). The GVBD is easily observed by the appearance of the white spot on the top of a *Xenopus* egg. We transcribed mRNAs from newly found *E. histolytica* kinase genes (*Eh chk2*, Eh1751, Eh1826 and Eh6121) and *Xenopus* β-actin gene as a negative control. Each mRNA was injected into interphase eggs, which were incubated for 12 h and stimulated with progesterone hormone to induce an entry into M phase of cell division. We counted the appearance of white spots and measured intervals where GVBD was observed in 50% eggs. The time of 50%-GVBD was 190–200 min in eggs uninjected and eggs injected with β-actin, Eh1826 or Eh6121 mRNAs, whereas, the time of 50%-GVBD was prolonged to over 420 min in eggs injected with *Eh chk2* mRNA (Fig. 3). To our surprise, the time of 50%-GVBD was prolonged also in eggs injected with Eh1751 mRNA, a homologue of RNA-dependent protein serine/threonine kinase (PKR) [27–29] (Fig. 3).

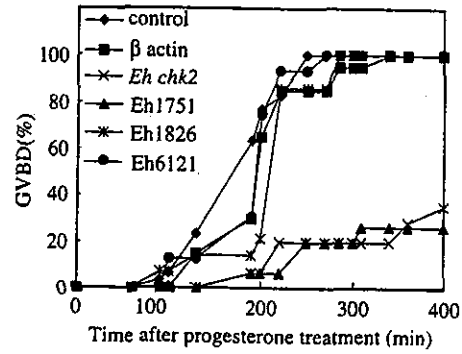

Fig. 3. *Eh chk2* mRNA induces a delay of cell division in *Xenopus* immature eggs. The mRNAs (6 ng each) encoding β-actin, *Eh chk2*, Eh1751, Eh1826 or Eh6121 were injected into 20 *Xenopus* eggs (control eggs were not injected). After progesterone treatment, the appearance of white spot in recipient eggs was counted at the indicated times. The percentage of the eggs, which showed white spot at the animal pole, was indicated as %GVBD.

Most vertebrate cells express both p42 MAPK (ERK2) and p44 MAPK (ERK1). In *Xenopus* eggs, however, only p42 MAPK is expressed. We then examined effects of *E. histolytica* kinases on activation of p42 MAPK and Cdc2, because both are phosphorylated and activated specifically in M phase of cell division [30]. Cellular proteins of eggs injected with those mRNAs were extracted and analyzed by western blotting. The protein bands of p42 MAPK were shifted up due to their phosphorylation and activation with the injections of β-actin, Eh1826 and Eh6121 mRNAs (Fig. 4, upper panel). Furthermore, the active forms of p42 MAPK were not detected in eggs injected with *Eh chk2*

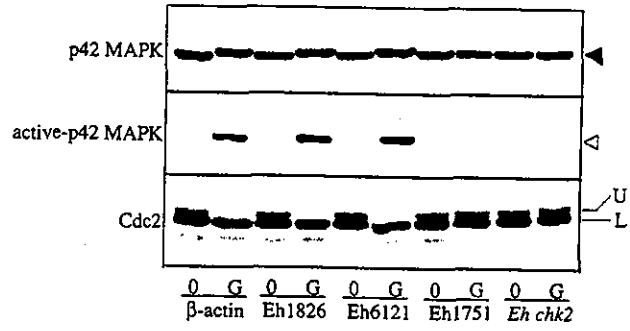

Fig. 4. Injection of *Eh chk2* mRNA delays the activations of p42 MAPK and Cdc2 kinase in *Xenopus* eggs. The eggs were injected with 6 ng of mRNAs of β-actin, Eh1826, Eh6121, Eh1751 or *Eh chk2* and treated with progesterone. The cellular proteins were collected just before progesterone treatment (represented as 0) and at 200 min after the treatment (G). GVBD was observed in about 50% of control eggs at 200 min. Total p42 MAPK was detected with anti-ERK 1/2 polyclonal antibody. The active forms of p42 MAPK and cdc2 kinase were detected with anti-phospho-p44/p42 MAPK (Thr-202/Tyr-204) E10 monoclonal antibody and anti-Cdc2 monoclonal antibody, respectively. The black arrow indicates both forms of activated and inactivated p42 MAPK. The white arrow indicates activated form of p42 MAPK. The upper band (U) of Cdc2 protein corresponds to the Tyr-15-phosphorylated form (inactive form) and the lower band (L) to the unphosphorylated form including active form of Cdc2. The weak band below the L band corresponds to Cdk2, a member of Cdk family.

mRNA and Eh1751 mRNA before GVBD (Fig. 4, middle panel). As for Cdc2 activation, the upper bands of Cdc2 inactive form, which is phosphorylated both Tyr-15 and Thr-14, disappeared with the injections of β-actin, Eh1826 and Eh6121 mRNAs, but not disappeared with the injections with *Eh chk2* mRNA and Eh1751 mRNA (Fig. 4, lower pannel). Therefore, *Eh chk2* mRNA and Eh1751 mRNA delayed the activation of both Cdc2 and p42 MAPK, whereas other *E. histolytica* kinase mRNAs did not show the effects. These results indicate that the *Eh chk2* gene has the function to prolong cell division in vivo and that the *Eh chk2* gene probably works in *E. histolytica* as a regulator of cell division as well as the human *chk2* gene.

4. Discussion

The life cycle of protozoan parasites, *E. histolytica*, has two stages; dormant cyst and amoebic trophozoite. The trophozoite proliferates by mitotic cell division and plays an essential role in amoebic diseases, although its growth regulation is not fully understood at the molecular levels. Identification of cell cycle regulator of *E. histolytica* will be helpful to control the amebiasis. We found six new genes of *E. histolytica* kinases including *Eh chk2*, a human *chk2* homologue in silico analysis. The human Chk2 plays a central role in G2 phase arrest of cell cycle by inhibiting Cdc25 phosphatase. Overexpression of human *chk2* (Cds1) gene was reported to delay the cell division in *Xenopus* eggs [31]. We showed that *Eh chk2* mRNA delayed the cell division in *Xenopus* eggs, whereas mRNAs of *Xenopus* β-actin or two other *E. histolytica* kinases did not (Fig. 3). In addition, *Eh chk2* mRNA inhibited p42 MAPK activation and Cdc2 activation, both of which are accompanied with cell division (Fig. 4). Our results indicate that the *Eh chk2* gene has similar functions to the human *chk2* gene.

The predicted amino acid sequence of *Eh chk2* contains a FHA domain in its N-terminal region. FHA domain is a protein–protein interaction motif which is widely found in checkpoint kinases of prokaryotes and eukaryotes. Rad53, a homologue of Chk2 kinase in a yeast *S. cerevisiae*, has two FHA domains and works in response to DNA damage [32–34]. The FHA domain in human Chk2 (Cds1) is indispensable region for its function [35]. The fact that predicted *Eh chk2* protein contains a FHA domain with highly conserved amino acid residues supports its functions are similar to human Chk2.

Interestingly, the injection of Eh1751 mRNA induced delay of cell division, and inhibited activation of p42 MAPK and Cdc2 in *Xenopus* eggs as well as injection of *Eh chk2* mRNA. DNA sequence of Eh1751 gene has homology to PKR kinase (interferon-induced double-stranded RNA-dependent kinase) (TIK). The expression of PKR is controlled in cell division. PKR is a potent inhibitor of cell growth in mammalian cells [36]. Our results suggest that Eh1751 is a PKR gene in *E. histolytica*.

We assessed the activity of *Eh chk2* gene in frog eggs in this report. The frog egg is a common system for examining functions of cell-cycle regulator genes in eukaryotes. However, more conclusive functions of *Eh chk2* gene should be confirmed in *E. histolytica* trophozoites. Over-expression or knockout of *Eh chk2* gene in the trophozoites will further clarify its biological functions [37–41]. It is known that the human Chk2 protein directly interacts with Cdc25 and inhibits its function, and the Chk2 is phosphorylated and activated by a check point kinase ATM [11–13]. Interaction between amoebic Cdc25 and Eh chk2 protein and requirement of ATM kinase for the activity of Eh chk2 will be interesting to be studied on. The identification and functional analysis of cell-cycle regulating genes of *E. histolytica* may give us a new resolution of amebiasis in the future.

Acknowledgements

We thank the Institute for Genomic Research (TIGR) for opening the *Entamoeba histolytica* Genome Database (http://www.tigr.org/tdb/e2k1/eha1/). TIGR informs that preliminary sequence data for *E. histolytica* is deposited regularly into the GSS division of GenBank and that the sequencing effort is part of the International *Entamoeba* Genome Sequencing Project and is supported by award from the National Institute of Allergy and Infectious Diseases, National Institutes of Health. Our work was supported in part by Grant-in-Aid for Scientific Research from the Ministry of Education, Science and Culture of Japan (No. 12780542).

References

[1] Haque R, Huston CD, Hughes M, Houpt E, Petri Jr WA. Amebiasis. N Engl J Med 2003;348(16):1565–73.
[2] Stanley Jr SL. Amoebiasis. Lancet 2003;361(9362):1025–34.
[3] WHO. Bull World Health Organ 1997;75:291–2.
[4] Masui Y, Markert CL. Cytoplasmic control of nuclear behavior during meiotic maturation of frog oocytes. J Exp Zool 1971;177:129–45.
[5] Lee MG, Nurse P. Complementation used to clone a human homologue of the fission yeast cell cycle control gene cdc2. Nature 1987;327:31–5.
[6] Nurse P. Universal control mechanism regulating onset of M-phase. Nature 1990;344:503–8.
[7] Murray AW, Solomon MJ, Kirschner MW. The role of cyclin synthesis and degradation in the control of maturation promoting factor activity. Nature 1989;339:280–6.
[8] Nurse P. Universal control mechanism regulating onset of M-phase. Nature 1990;344:503–8.
[9] Sadhu K, Reed SI, Richardson H, Russell P. Human homolog of fission yeast cdc25 mitotic inducer is predominantly expressed in G2. Proc Natl Acad Sci U S A 1990;87:5139–43.
[10] Walworth N, Davey S, Beach D. Fission yeast chk1 protein kinase links the rad checkpoint pathway to cdc2. Nature 1993;363:368–71.
[11] Matsuoka S, Huang M, Elledge SJ. Linkage of ATM to cell cycle regulation by the *Chk2* protein kinase. Science 1998;282:1893–7.

[12] Matsuoka S, Rotman G, Ogawa A, Shiloh Y, Tamai K, Elledge SJ. Ataxia telangiectasia-mutated phosphorylates Chk2 in vivo and in vitro. Proc Natl Acad Sci U S A 2000;97:10389–94.

[13] Hirao A, Kong YY, Matsuoka S, Wakeham A, Ruland J, Yoshida H, et al. DNA damage-induced activation of p53 by the checkpoint kinase Chk2. Science 2000;287:1824–7.

[14] Lohia A, Samuelson J. Cloning of the *Eh* cdc2 gene from *Entamoeba histolytica* encoding a protein kinase p34cdc2 homologue. Gene 1993; 127:203–7.

[15] Shen PS, Lohia A, Samuelson J. Molecular cloning of ras and rap genes from *Entamoeba histolytica*. Mol Biochem Parasitol 1994; 64:111–20.

[16] Lohia A, Samuelson J. Molecular cloning of a rho family gene of *Entamoeba histolytica*. Mol Biochem Parasitol 1993;58:177–80.

[17] Lohia A, Samuelson J. Molecular cloning of an *Entamoeba histolytica* gene encoding a putative mos family serine/threonine-kinase. Biochim Biophys Acta 1994;1222(1):122–4.

[18] Marmur J. A procedure for the isolation of deoxyribonucleic acid from microorganism. J Mol Biol 1996;3:208–18.

[19] Diamond LS, Harlow DR, Cunnick CC. A new medium for the axenic cultivation of *Entamoeba histolytica* and other *Entamoeba*. Trans R Soc Trop Med Hyg 1978;72:431–2.

[20] Kozak M. Point mutations define a sequence flanking the AUG initiator codon that modulates translation by eukaryotic ribosomes. Cell 1986;44:283–92.

[21] Furuno N, Nishizawa M, Okazaki K, Tanaka H, Iwashita J, Nakajo N, et al. Suppression of DNA replication via Mos function during meiotic divisions in *Xenopus* oocytes. EMBO J 1994;13(10):2399–410.

[22] Sagata N, Watanabe N, Vande Woude GF, Ikawa Y. The c-mos proto-oncogene product is a cytostatic factor responsible for meiotic arrest in vertebrate eggs. Nature 1989;342(6249):483–4.

[23] Laemmli UK. Cleavage of structural proteins during the assembly of the head of bacteriophage T4. Nature 1970;227:680–5.

[24] Sun Z, Hsiao J, Fay DS, Stern DF. Rad53 FHA domain associated with phosphorylated Rad9 in the DNA damage checkpoint. Science 1998;281(5374):272–4.

[25] Durocher D, Henckel J, Fersht AR, Jackson SP. The FHA domain is a modular phosphopeptide recognition motif. Mol Cell 1999;4(3): 387–94.

[26] Hofmann K, Bucher P. The FHA domain: a putative nuclear signalling domain found in protein kinases and transcription factors. Trends Biochem Sci 1995;20(9):347–9.

[27] Baier LJ, Shors T, Shors ST, Jacobs BL. The mouse antiphosphotyrosine immunoreactive kinase, TIK, is indistinguishable from the double-stranded RNA-dependent, interferon-induced protein kinase, PKR. Nucleic Acids Res 1993;21(20):4830–5.

[28] Langland JO, Jacobs BL. The role of the PKR-inhibitory genes, E3L and K3L, in determining vaccinia virus host range. Virology 2002;299(1):133–41.

[29] Auch C, Saha RNJ, Sheikh FG, Liu X, Jacobs BL, Pahan K. Role of protein kinase R in double-stranded RNA-induced expression of nitric oxide synthase in human astroglia. FEBS Lett 2004;563(1–3):223–8.

[30] James E, Ferrell Jr JE. *Xenopus* oocyte maturation: new lessons from a good egg. 1999;21(10):833–42.

[31] Gotoh T, Ohsumi K, Matsui T, Takisawa H, Kishimoto T. Inactivation of the checkpoint kinase Cds1 is dependent on cyclin B-Cdc2 kinase activation at the meiotic G(2)/M-phase transition in *Xenopus* oocytes. J Cell Sci 2001;14:3397–406.

[32] Chehab NH, Malikzay A, Appel M, Halazonetis TD. Chk2/hCds1 functions as a DNA damage checkpoint in G(1) by stabilizing p53. Genes Dev 2000;14(3):278–88.

[33] Hirao A, Kong YY, Matsuoka S, Wakeham A, Ruland J, Yoshida H, et al. DNA damage-induced activation of p53 by the checkpoint kinase Chk2. Science 2000;287(5459):1824–7.

[34] Liao H, Yuan C, Su MI, Yongkiettrakul S, Qin D, Li H, et al. Structure of the FHA1 domain of yeast Rad53 and identification of binding sites for both FHA1 and its target protein Rad9. J Mol Biol 2000; 304(5):941–51.

[35] Lee CH, Chung JH. The hCds1 (Chk2)-FHA domain is essential for a chain of phosphorylation events on hCds1 that is induced by ionizing radiation. J Biol Chem 2001;276(32):30537–41.

[36] Zamanian-Daryoush M, Der SD, Williams BR. Cell cycle regulation of the double stranded RNA activated protein kinase, PKR. Oncogene 1999;18(2):315–26.

[37] Hellberg A, Nickel R, Lotter H, Tannich E, Bruchhaus I. Over-expression of cysteine proteinase 2 in *Entamoeba histolytica* or *Entamoeba dispar* increases amoeba-induced monolayer destruction in vitro but does not augment amoebic liver abscess formation in gerbils. Cell Microbiol 2001;3(1):13–20.

[38] Nozaki T, Asai T, Sanchez LB, Kobayashi S, Nakazawa M, Takeuchi T. Characterization of the gene encoding serine acetyltransferase, a regulated enzyme of cysteine biosynthesis from the protist parasites *Entamoeba histolytica* and *Entamoeba dispar*. Regulation and possible function of the cysteine biosynthetic pathway in *Entamoeba*. J Biol Chem 1999;274(45):32445–52.

[39] Bracha R, Nuchamowitz Y, Leippe M, Mirelman D. Antisense inhibition of amoebapore expression in *Entamoeba histolytica* causes a decrease in amoebic virulence. Mol Microbiol 1999;34(3):463–72.

[40] Ankri S, Padilla-Vaca F, Stolarsky T, Koole L, Katz U, Mirelman D. Antisense inhibition of expression of the light subunit (35 kDa) of the Gal/GalNac lectin complex inhibits *Entamoeba histolytica* virulence. Mol Microbiol 1999;33(2):327–37.

[41] Arhets P, Olivo JC, Gounon P, Sansonetti P, Guillen N. Virulence and functions of myosin II are inhibited by overexpression of light meromyosin in *Entamoeba histolytica*. Mol Biol Cell 1998;9(6): 1537–47.

CLINICAL AND DIAGNOSTIC LABORATORY IMMUNOLOGY, Nov. 2004, p. 1085–1088 Vol. 11, No. 6
1071-412X/04/$08.00+0 DOI: 10.1128/CDLI.11.6.1085–1088.2004
Copyright © 2004, American Society for Microbiology. All Rights Reserved.

Improved Affinity of a Human Anti-*Entamoeba histolytica* Gal/GalNAc Lectin Fab Fragment by a Single Amino Acid Modification of the Light Chain

Hiroshi Tachibana,[1]* Naohisa Matsumoto,[1] Xun-Jia Cheng,[1] Hideo Tsukamoto,[2] and Eisaku Yoshihara[3]

Departments of Infectious Diseases[1] and Molecular Life Sciences[3] and Laboratory for Molecular Science Research,[2] Tokai University School of Medicine, Isehara, Kanagawa, Japan

Received 18 August 2004/Returned for modification 2 September 2004/Accepted 9 September 2004

We previously produced, in *Escherichia coli*, a human monoclonal antibody Fab fragment, CP33, specific for the galactose- and *N*-acetyl-D-galactosamine-inhibitable lectin of *Entamoeba histolytica*. To prepare antibodies with a higher affinity to the lectin, recombination PCR was used to exchange Ser^{91} and Arg^{96} in the third complementarity-determining region of the light chain with other amino acids. The screening of 200 clones of each exchange by an indirect fluorescent antibody test showed that 14 clones for Ser^{91} and nine clones for Arg^{96} reacted strongly with *E. histolytica* trophozoites. Sequence analyses revealed that the substituted amino acids at Ser^{91} were Ala in five clones, Gly in three clones, Pro in two clones, and Val in two clones, while the amino acid at position 96 was substituted with Leu in three clones. The remaining eight clones exhibited no amino acid change at position 91 or 96. These mutant Fab fragments were purified and subjected to a surface plasmon resonance assay to measure the affinity of these proteins to the cysteine-rich domain of lectin. Pro or Gly substitution for Ser^{91} caused an increased affinity of the Fab, but substitution with Ala or Val did not. The replacement of Arg^{96} with Leu did not affect affinity. These results demonstrate that modification of antibody genes by recombination PCR is a useful method for affinity maturation and that amino acid substitution at position 91 yields Fabs with increased affinity for the lectin.

Amebiasis caused by infection with the intestinal protozoan parasite *Entamoeba histolytica* is a notable parasitic disease in both developing and developed countries. It has been estimated that 50 million people develop amebic colitis and extraintestinal abscesses, resulting in up to 110,000 deaths annually (18). The development of immunoprophylaxis and accurate diagnostic tools is important for the control of amebiasis. The application of monoclonal antibodies is a promising avenue of research for improvement in diagnosis.

We recently produced several human monoclonal antibody Fab fragments specific for *E. histolytica* in *Escherichia coli* by use of combinatorial immunoglobulin gene libraries constructed from the peripheral lymphocytes of a patient with an amebic liver abscess and from an asymptomatic cyst passer (1, 14, 17). One of the Fab clones, CP33, derived from the asymptomatic cyst passer, recognized the cysteine-rich domain of the heavy subunit of the galactose- and *N*-acetyl-D-galactosamine-inhibitable (Gal/GalNAc) lectin (12) of *E. histolytica* (17). This clone exhibited neutralizing activities to amebic adherence and to erythrophagocytosis. Furthermore, we produced the Fab fragment fused with alkaline phosphatase for diagnostic purposes (16).

Recombinant antibody technology makes it possible to introduce site-directed or random mutations in the original antibody gene (3–5, 13, 19). Residues in the complementarity-determining region (CDR), especially in CDR3 of both the heavy and light chains of antibody, are considered responsible for high-energy interactions with antigen. Therefore, mutations at these residues will likely abolish antigen binding. However, an increased affinity may also occur by mutation if the native residue exhibits a negative effect on the interaction. In the Kabat numbering system, CDR3 of the light chain is the amino acid segment from position 89 to 97 (6, 20). The corresponding amino acid residues in CP33 were GlnGlnSerTyrSer ThrProArgThr (17). When an additional 13 light chains which constitute antilectin Fabs with the heavy chain of CP33 were analyzed, high variability was observed at positions 91, 92, 94, and 96 (17). As a first step in the affinity maturation of human antibodies to *E. histolytica*, we attempted to modify Fab clone CP33 by single-amino-acid substitutions of Ser^{91} and Arg^{96} in the light chain.

MATERIALS AND METHODS

Site-directed mutagenesis. Site-directed mutagenesis in the light chain gene of CP33 (17) was performed by recombination PCR (7). The plasmid vector pFab1-His2, containing the light and the Fd region of the heavy chain genes, was amplified by using two sets of primers, CP33L-S^{91}X-For (5′-CAACTTACTAC TGTCAACAGNNNTACAGTAC-3′, where N is any nucleotide) and CP33L-S^{91}-Rev (5′-CTGTTGACAGTAGTAAGTTGCAAAATCTTC-3′), and CP33L-R^{96}X-For (5′-AACAGAGTTACAGTACCCCTNNNACCTTCGG-3′) and CP33L-R^{96}-Rev (5′-AGGGGTACTGTAACTCTGTTGACAGTAGTAAG-3′). The positions of these primers in the light-chain gene of CP33 are shown in Fig. 1.

To obtain high fidelity amplification, *Pyrobest* DNA polymerase (Takara, Otsu, Japan) was used. Twenty-five cycles of PCR were performed as follows: denaturation at 94°C for 15 s (135 s in cycle 1), annealing at 60°C for 30 s, and polymerization at 72°C for 360 s. The PCR products were purified by agarose gel electrophoresis and by use of a Qiaex II gel extraction kit (Qiagen GmbH, Hilden, Germany). The DNA fragments were introduced into *E. coli* JM109 cells.

* Corresponding author. Mailing address: Department of Infectious Diseases, Tokai University School of Medicine, Isehara, Kanagawa 259-1193, Japan. Phone: 81 (463) 93-1121. Fax: 81 (463) 95-5450. E-mail: htachiba@is.icc.u-tokai.ac.jp.

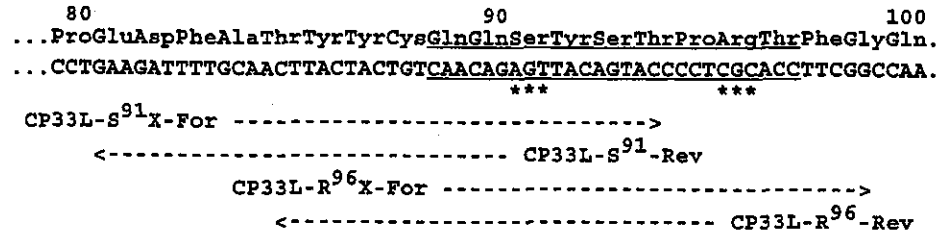

FIG. 1. Positions of the four primers used in recombination PCR of the light-chain gene of CP33. The partial nucleotide sequence and the deduced amino acid sequence of the light-chain gene are shown. Numbers above the sequence indicate amino acid positions in the Kabat numbering system. CDR3 is underlined. The locations of the nucleotides where mutations were introduced are indicated by asterisks. Dashed lines and arrowheads indicate the corresponding sites and directions of the primers.

Expression of Fabs and screening. Bacterial expression of Fabs was performed essentially as previously described (14). Each clone was cultured in 2 ml of super broth (30 g of tryptone, 20 g of yeast extract, 10 g of morpholinepropanesulfonic acid per liter [pH 7]) containing ampicillin until an optical density at 600 nm of 0.4 to 0.6 was achieved. Isopropyl-β-D-thiogalactopyranoside (IPTG) was added to the bacterial cultures to a final concentration of 0.1 mM, and the cells were then cultured for a further 12 h at 30°C. The cells were harvested by centrifugation, suspended in 150 μl of phosphate-buffered saline (PBS, pH 7.2) containing 1 mM phenylmethylsulfonyl fluoride, and then ruptured by sonication. After centrifugation of the lysates at 18,000 × *g* for 10 min, the supernatant was screened by an indirect fluorescent antibody test.

Indirect fluorescent antibody test. Trophozoites of *E. histolytica* HM-1:IMSS were cultured axenically in BI-S-33 medium (2) supplemented with 10% adult bovine serum at 37°C. Trophozoites of *Entamoeba dispar* SAW1734RclAR were cultured monoxenically with *Pseudomonas aeruginosa* in BCSI-S medium at 37°C (9). These trophozoites at the logarithmic phase of growth were used in the following experiments. The indirect fluorescent antibody test was performed with formalin-fixed trophozoites as described previously (15). Fluorescein isothiocyanate-conjugated goat immunoglobulin G to human immunoglobulin G Fab (ICN Pharmaceuticals, Aurora, Ohio) was used as the secondary antibody.

For confocal laser scanning microscopy, *E. histolytica* trophozoites were transferred onto glass coverslips in a culture dish containing medium and incubated for 2 h at 37°C. After removal of the medium, the coverslips were incubated in PBS containing 4% paraformaldehyde for 30 min. The trophozoites were washed with PBS and then permeabilized by treatment with 0.1% Triton X-100 for 5 min at room temperature. The trophozoites were again washed with PBS and blocked with 3% bovine serum albumin in PBS for 1 h at room temperature. Purified Fab was added, and the coverslips were incubated for 12 h at 4°C. The coverslips were washed with PBS and then incubated with the secondary antibody for 5 h at 4°C. The coverslips were again washed with PBS and then stained with 2.5 μg of propidium iodide per ml for 10 min at room temperature. We used an LM410 confocal laser scanning microscope (Carl Zeiss Vision GmbH, Hallbergmoos, Germany) to observe the samples.

DNA sequencing. Plasmid DNA was isolated from the indirect fluorescent antibody-positive clones. Light-chain genes in the expression vector were subcloned into sequencing vector. Sequencing in both directions was performed with a BigDye Terminator v3.1 cycle sequencing kit (Applied Biosystems, Foster City, Calif.) with M13 primers. The reactions were run on an ABI Prism 3100 genetic analyzer (Applied Biosystems).

Purification of Fabs. Selected positive clones were cultured in 400 ml of medium. The cells were disrupted and the supernatant was prepared as described above. Purification of Fabs in the supernatant was achieved by affinity chromatography with His•Bind resin (Novagen, Madison, Wis.) according to the manufacturer's instructions.

Sodium dodecyl sulfate-polyacrylamide gel electrophoresis. Purified Fabs were solubilized with an equal volume of sample buffer (10) containing 2 mM phenylmethylsulfonyl fluoride, 2 mM *N*-α-*p*-tosyl-L-lysine chloromethyl ketone, and 4 μM leupeptin for 5 min at 95°C and then subjected to sodium dodecyl sulfate-polyacrylamide gel electrophoresis under reducing conditions.

Determination of affinity constants. The affinity constants of Fabs were assessed by surface plasmon resonance with the BIAcore 3000 instrument (Biacore AB, Uppsala, Sweden), according to the general procedure outlined by the manufacturer (8). The cysteine-rich domain of the Gal/GalNAc lectin heavy subunit, rLecA (11), kindly provided by W. A. Petri, Jr., University of Virginia, was immobilized onto a CM5 chip (Biacore) surface at a low density by amine coupling chemistry. Association and dissociation constants were determined by using the software of the manufacturers, BIAevaluation 3.1.

RESULTS

Amino acid modifications at positions 91 and 96. Transformation of *E. coli* with two kinds of PCR products yielded more than 10^4 colonies. Of these, 200 clones of each exchange were randomly selected and then cultured for the expression of Fabs. When *E. coli* extracts from those clones with a randomly mutated amino acid at position 91 were screened to detect Fab fragments reactive with formalin-fixed *E. histolytica* trophozoites, 37 positive samples were obtained. In the second screening, 10-fold-diluted samples of the *E. coli* extracts were also examined by indirect fluorescent antibody test. Fourteen samples were found to be strongly reactive with the *E. histolytica* trophozoites, which was comparable to the reactivity of the original clone CP33. Sequencing of the light-chain genes revealed that Ser^{91} of the light chain had been replaced by Ala in five clones, Gly in three clones, Pro in two clones, and Val in two clones. The remaining two clones showed no substitution at this amino acid, although the nucleotide sequences were changed. Interestingly, these four residues are grouped into the amino acids with nonpolar side chains. On the other hand, when the mutations were introduced at Arg^{96}, nine clones were shown to be reactive with the *E. histolytica* trophozoites as strongly as the original clone CP33. Among these nine clones, three exhibited a replacement of Arg^{96} with Leu, while the other six showed no replacement.

Reactivity of the modified Fabs. We selected one clone from each group with the same mutation at Fab. These clones were cultured on a large scale to obtain Fab fragments to be purified by affinity chromatography for the His tag. Sodium dodecyl sulfate-polyacrylamide gel electrophoresis of the purified proteins demonstrated two bands with apparent molecular masses of 24 and 25 kDa under reduced conditions (data not shown). These purified Fabs were confirmed to be reactive with *E. histolytica* trophozoites by confocal laser scanning microscopy. Localization of bright fluorescence on the surface of the trophozoites was demonstrated by immunostaining with the modified antibody clones as well as with the unmodified antibody CP33 (data not shown). The specificity of the modified Fabs was also examined by indirect fluorescent antibody test. The Fabs were not reactive with *E. dispar*, indicating that amino acid modifications did not affect the specificity of these Fabs.

Affinity comparison of the modified Fabs. The affinity of the purified Fabs to the antigen was assessed by surface plasmon resonance. As shown in Table 1, the association and dissociation constant values of clone 1 without the amino acid substitution were comparable to the values of CP33 reported in a

TABLE 1. Association and dissociation constants of the binding of modified human Fab fragments to the cysteine-rich domain of the Gal/GalNAc lectin heavy subunit of *E. histolytica*, measured by surface plasmon resonance

Fab	Amino acid change in light chain		K_a (1/M)	Increase compared to CP33 (fold)	K_d (M)	Decrease compared to CP33 (fold)
	Ser^{91}	Arg^{96}				
Clone 1	Ser (AGC)		5.53×10^7	0.8	1.81×10^{-8}	0.8
Clone 2	Pro (CCA)		3.49×10^8	4.9	2.87×10^{-9}	4.8
Clone 3	Ala (GCG)		6.38×10^7	0.9	1.57×10^{-8}	0.9
Clone 4	Gly (GGC)		1.21×10^8	1.7	8.24×10^{-9}	1.7
Clone 5	Val (GTC)		7.64×10^7	1.1	1.88×10^{-8}	0.7
Clone 6		Leu (CTG)	4.95×10^7	0.7	2.02×10^{-8}	0.7
CP33[a]			7.19×10^7	1.0	1.39×10^{-8}	1.0

[a] These values are from a previous study (17).

previous paper (17). The affinity of the Fabs with $Ser^{91}Pro$ (clone 2) and $Ser^{91}Gly$ (clone 4) was found to be approximately 4.8- and 1.7-fold higher, respectively, than that of the original Fab. However, the mutants with $Ser^{91}Ala$ (clone 3) and $Ser^{91}Val$ (clone 5) exhibited dissociation constants comparable to those for clone 1 or CP33. On the other hand, the affinity of the Fab with $Arg^{96}Leu$ (clone 6) was comparable to that of CP33.

DISCUSSION

The present study demonstrated that a single-amino-acid replacement of Ser^{91} in CDR3 of the light chain could improve the affinity of CP33. A number of possible explanations for this observation occurred to us. First, the contribution of the Ser^{91} residue to the interaction between antigen and antibody was considered. Ser is a polar amino acid and therefore may contribute to binding affinity by forming a hydrogen bond to the amino acid of the lectin. However, this possibility is unlikely because hydrophobic amino acids such as Ala and Val are not able to form a hydrogen bond, but the substitution of Ser with Ala or Val appeared to have a lesser effect on the binding affinity of the antibody.

Second, it was considered that Ser^{91} might inhibit affinity through steric hindrance. The substitution of Ser with Pro leads to residue bending, which results in the conformational change which allowed the redistribution of the neighboring amino acids favoring the antigen-antibody interaction. The increased affinity of the antibody by the replacement of Ser with Gly supports the second consideration because Gly is the smallest amino acid and therefore is capable of reducing the steric hindrance caused by the Ser residue. Furthermore, this notion is consistent with the finding that the Ala and Val substitutions exhibited no effect on binding affinity because the sizes of Ala and Val residues are comparable to that of Ser. It is known that the effect of a mutation is not restricted to contact residues (19). Although the residue at position 91 may not react directly with antigenic molecules, it can affect the binding of residue 93 (5). Therefore, the second possibility seems more likely to be the explanation, although we cannot exclude other possibilities.

In contrast, improvement of affinity was not achieved by the single-amino-acid modification at Arg^{96}. Since the amino acid change from Arg to Leu is thought to be drastic, it is reasonable to expect a distinct change in binding affinity. However, this was not the case. At present, the reason is not clear. As the nucleotide sequence has not been analyzed in all clones, there is the possibility that substitutions to amino acids translated from only one genetic code were not included in the mutagenesis of this study. However, since 200 clones were examined, the probability that the Met and Trp substitutions were not included is theoretically less than 0.2%. Therefore, it appears that Arg may be the best residue in this position on the light chain.

To our knowledge, this is the first report demonstrating the modification of antibody genes by recombination PCR. Single-amino-acid substitution by this method demonstrated the feasibility of improving the affinity of the original human Fab. Further studies on modification of other residues in CDR3, including residues that contact the antigen, will contribute to improve the affinity of the human antibody and thereby improve its utility for diagnosis and immunoprophylaxis.

ACKNOWLEDGMENTS

We thank W. A. Petri, Jr., for generously supplying the recombinant lectin.

This work was supported by a Grant-in-Aid for Scientific Research from the Japanese Society for the Promotion of Science and grants from the Ministry of Health, Labour and Welfare of Japan. X.-J.C. is a recipient of the Japanese Society for the Promotion of Science Postdoctoral Fellowship for Foreign Researchers.

REFERENCES

1. **Cheng, X. J., S. Ihara, M. Takekoshi, and H. Tachibana.** 2000. *Entamoeba histolytica*: bacterial expression of a human monoclonal antibody which inhibits in vitro adherence of trophozoites. Exp. Parasitol. **96**:52–56.
2. **Diamond, L. S., D. R. Harlow, and C. C. Cunnick.** 1978. A new medium for the axenic cultivation of *Entamoeba histolytica* and other *Entamoeba*. Trans. R. Soc. Trop. Med. Hyg. **72**:431–432.
3. **Dong, L., S. Chen, U. Bartsch, and M. Schachner.** 2003. Generation of affinity matured scFv antibodies against mouse neural cell adhesion molecule L1 by phage display. Biochem. Biophys. Res. Commun. **301**:60–70.
4. **Fujii, I.** 2004. Antibody affinity maturation by random mutagenesis. Methods Mol. Biol. **248**:345–359.
5. **Hall, B. L., H. Zaghouani, C. Daian, and C. A. Bona.** 1992. A single amino acid mutation in CDR3 of the 3–14–9 L chain abolished expression of the IDA 10-defined idiotope and antigen binding. J. Immunol. **149**:1605–1612.
6. **Johnson, G., and T. T. Wu.** 2004. The Kabat database and a bioinformatics example. Methods Mol. Biol. **248**:11–25.
7. **Jones, D. H., and S. C. Winistorfer.** 1997. Recombination and site-directed mutagenesis using recombination PCR. Methods Mol. Biol. **67**:131–140.
8. **Karlsson, R., and A. Larsson.** 2004. Affinity measurement using surface plasmon resonance. Methods Mol. Biol. **248**:389–415.
9. **Kobayashi, S., E. Imai, H. Tachibana, T. Fujiwara, and T. Takeuchi.** 1998. *Entamoeba dispar*: cultivation with sterilized *Crithidia fasciculata*. J. Eukaryot. Microbiol. **45**:3S–8S.
10. **Laemmli, U. K.** 1970. Cleavage of structural proteins during the assembly of the head of bacteriophage T4. Nature **227**:680–685.
11. **Mann, B. J., C. Y. Chung, J. M. Dodson, L. S. Ashley, L. L. Braga, and T. L. Snodgrass.** 1993. Neutralizing monoclonal antibody epitopes of the *Entam-*

oeba histolytica galactose adhesin map to the cysteine-rich extracellular domain of the 170-kilodalton subunit. Infect. Immun. **61**:1772–1778.

12. **Petri, W. A., Jr., R. Haque, and B. J. Mann.** 2002. The bittersweet interface of parasite and host: lectin-carbohydrate interactions during human invasion by the parasite *Entamoeba histolytica*. Annu. Rev. Microbiol. **56**:39–64.
13. **Sharon, J.** 1990. Structural correlates of high antibody affinity: three engineered amino acid substitutions can increase the affinity of an anti-p-azophenylarsonate antibody 200-fold. Proc. Natl. Acad. Sci. USA **87**:4814–4817.
14. **Tachibana, H., X. J. Cheng, K. Watanabe, M. Takekoshi, F. Maeda, S. Aotsuka, Y. Kaneda, T. Takeuchi, and S. Ihara.** 1999. Preparation of recombinant human monoclonal antibody Fab fragments specific for *Entamoeba histolytica*. Clin. Diagn. Lab. Immunol. **6**:383–387.
15. **Tachibana, H., S. Kobayashi, Y. Kato, K. Nagakura, Y. Kaneda, and T. Takeuchi.** 1990. Identification of a pathogenic isolate-specific 30,000-M_r antigen of *Entamoeba histolytica* by using a monoclonal antibody. Infect. Immun. **58**:955–960.
16. **Tachibana, H., M. Takekoshi, X. J. Cheng, Y. Nakata, T. Takeuchi, and S. Ihara.** 2004. Bacterial expression of a human monoclonal antibody-alkaline phosphatase conjugate specific for *Entamoeba histolytica*. Clin. Diagn. Lab. Immunol. **11**:216–218.
17. **Tachibana, H., K. Watanabe, X. J. Cheng, H. Tsukamoto, Y. Kaneda, T. Takeuchi, S. Ihara, and W. A. Petri, Jr.** 2003. VH3 gene usage in neutralizing human antibodies specific for the *Entamoeba histolytica* Gal/GalNAc lectin heavy subunit. Infect. Immun. **71**:4313–4319.
18. **Walsh, J. A.** 1986. Problems in recognition and diagnosis of amebiasis: estimation of the global magnitude of morbidity and mortality. Rev. Infect. Dis. **8**:228–238.
19. **Winkler, K., A. Kramer, G. Kuttner, M. Seifert, C. Scholz, H. Wessner, J. Schneider-Mergener, and W. Hohne.** 2000. Changing the antigen binding specificity by single point mutations of an anti-p24 (HIV-1) antibody. J. Immunol. **165**:4505–4514.
20. **Wu, T. T., and E. A. Kabat.** 1970. An analysis of the sequences of the variable regions of Bence Jones proteins and myeloma light chains and their implications for antibody complementarity. J. Exp. Med. **132**:211–250.

JOURNAL OF CLINICAL MICROBIOLOGY, Mar. 2004, p. 1069–1074 Vol. 42, No. 3
0095-1137/04/$08.00+0 DOI: 10.1128/JCM.42.3.1069–1074.2004
Copyright © 2004, American Society for Microbiology. All Rights Reserved.

Evaluation of Recombinant Fragments of *Entamoeba histolytica* Gal/GalNAc Lectin Intermediate Subunit for Serodiagnosis of Amebiasis

Hiroshi Tachibana,[1]* Xun-Jia Cheng,[1,2] Gohta Masuda,[3]† Noriyuki Horiki,[4,5] and Tsutomu Takeuchi[6]

Department of Infectious Diseases, Tokai University School of Medicine, Isehara, Kanagawa,[1] Tokyo Metropolitan Komagome Hospital, Bunkyo-ku,[3] Division of Internal Medicine, St. Luke's International Hospital, Chuo-ku,[5] and Department of Tropical Medicine and Parasitology, Keio University School of Medicine, Shinjuku-ku,[6] Tokyo, and Third Department of Internal Medicine, Mie University School of Medicine, Tsu, Mie,[4] Japan, and Department of Medical Microbiology and Parasitology, Fudan University School of Medicine, Shanghai, China[2]

Received 18 September 2003/Returned for modification 10 November 2003/Accepted 24 November 2003

We have recently identified a 150-kDa surface antigen of *Entamoeba histolytica* as an intermediate subunit (Igl) of galactose- and *N*-acetyl-D-galactosamine-inhibitable lectin, which is a cysteine-rich protein consisting of 1,101 amino acids (aa) and containing multiple CXXC motifs in amino acid sequences. In the present study, full-length Igl except for the signal sequences (aa 14 to 1088) and three fragments of Igl—the N-terminal part (aa 14 to 382), the middle part (aa 294 to 753), and the C-terminal part (aa 603 to 1088)—were prepared in *Escherichia coli*, and the reactivity of these recombinant proteins with sera from patients with amebiasis was examined by means of enzyme-linked immunosorbent assay (ELISA). Sera from 57 symptomatic patients with amebic liver abscess or amebic colitis, sera from 15 asymptomatic cyst passers, sera from 40 individuals with other protozoan infections, and sera from 50 healthy controls were used. The sensitivity and specificity of the recombinant full-length Igl in the ELISA were 90 and 94%, respectively. When three fragments were used as antigens in the ELISA, the sensitivities were 56% in the N terminus, 92% in the middle part, and 97% in the C terminus. The specificities of the three antigens were 96% in the N terminus and 99% in both the middle and C-terminal fragments. These results demonstrate that Igl is well recognized in not only symptomatic but also asymptomatic patients with *E. histolytica* infection and that the carboxyl terminus of Igl is an especially useful antigen for the serodiagnosis of amebiasis.

Amebiasis caused by infection with *Entamoeba histolytica* is an important parasitic disease in both developing and developed countries. It has been estimated that *E. histolytica* causes 50 million cases of colitis and liver abscess, resulting in 40,000 to 110,000 deaths annually (27). In cases of liver abscesses, diagnosis and treatment at an early stage are required to prevent fatal infection. Whereas the detection of trophozoites in liver pus is not easy, a serological test is practical as a sensitive and noninvasive means of diagnosis of amebic liver abscess (11, 21). On the other hand, in cases of asymptomatic cyst passers, *E. histolytica* and *E. dispar*, which is a nonpathogenic commensal ameba, must be distinguished by PCR analysis or by the detection of *E. histolytica*-specific antigens (2). However, since positive serology is found in most asymptomatic cases infected with *E. histolytica*, serological tests are also applicable (24). Thus, serodiagnosis is an important laboratory diagnostic tool for amebiasis, as well as microscopic detection of the pathogen.

Recently, several recombinant *E. histolytica* antigens were prepared, and their usefulness for serodiagnosis has been reported (12, 14, 18–20, 22, 28). One of the useful antigens is the 170-kDa heavy subunit (Hgl) of galactose- and *N*-acetyl-D-galactosamine-inhibitable lectin, which is the key factor in amebic adherence and subsequent pathogenesis (16). Hgl is a transmembrane protein that assumes a heterodimeric conformation that conforms with glycosylphosphatidylinositol (GPI)-anchored 31/35-kDa light subunit by disulfide bonds (15). We recently identified a GPI-anchored 150-kDa intermediate subunit (Igl) of lectin, which is noncovalently associated with Hgl (4, 8). A mouse monoclonal antibody specific for Igl significantly inhibits adherence and cytotoxicity of trophozoites to mammalian cells, erythrophagocytosis, and liver abscess formation in hamsters (5, 7, 23). Igl is a cysteine-rich protein that consists of 1,101 amino acids (aa) and contains multiple CXXC motifs in amino acid sequences (4). In the previous study, we examined the reactivity of sera from ameba-infected patients to affinity purified Igl by Western immnoblot analysis. The native Igl was recognized by all sera from not only symptomatic patients but also asymptomatic cyst passers (8). However, the possibility that copurified Hgl might affect the reactivity of Igl could not be excluded. Therefore, in the present study, recombinant Igl was prepared in *Esherichia coli*, and its reactivity with sera from patients with amebiasis was examined. We also report here on the different reactivity of partial Igl fragments with the sera.

* Corresponding author. Mailing address: Department of Infectious Diseases, Tokai University School of Medicine, Bohseidai, Isehara, Kanagawa 259-1193, Japan. Phone: 81 (463) 93-1121. Fax: 81 (463) 95-5450. E-mail: htachiba@is.icc.u-tokai.ac.jp.

† Present address: Tokyo Metropolitan Kita Medical and Rehabilitation Center, Kita-ku, Tokyo, Japan.

MATERIALS AND METHODS

Plasmid constructs for recombinant proteins. The DNA fragment coding for the full-length Igl, except for the N terminus and C terminus signal sequences

TABLE 1. List of oligonucleotide primers used in this study

Primer	Positions[a]	Sequence (5′ to 3′)[b]
EhIgl-S14	40–59	CCCTCGAGGATTATACTGCTGATAAGCT
EhIgl-S294	880–898	CCCTCGAGACAGAAGAAAATAAATGTA
EhIgl-AS382	1129–1146	CCCTCGAGTTAAAGTTTGCATGGTCCATC
EhIgl-S603	1807–1827	CCCTCGAGGAAGGACCAAATGCAGAAGAT
EhIgl-AS753	2244–2259	CCCTCGAGTTATAGCCTTTGTTCAGTG
EhIgl-AS1088	3247–3264	CCCTCGAGTTAAATGCCTTTAGCTCCATT

[a] Nucleic acid numbering is based on the *E. histolytica* Igl1 gene sequence (AF337950).

[b] Nucleotides added for cloning and translation termination are underlined.

(F-Igl, aa 14 to 1088 of *E. histolytica* Igl1), was obtained by PCR amplification of a plasmid containing the gene encoding Igl1 of *E. histolytica* HM-1:IMSS strain (4). DNA fragments, coding for three overlapping parts of Igl—the N-terminal part (N-Igl, aa 14 to 382), the middle part (M-Igl, aa 294 to 753), and the C-terminal part (C-Igl, aa 603 to 1088)—were also amplified by PCR. The oligonucleotide primers used are listed in Table 1. Twenty cycles of PCR were performed as follows: denaturation at 94°C for 15 s (135 s in cycle 1), annealing at 55°C for 30 s, and polymerization at 72°C for 60 s (360 s in cycle 20). Each of the amplified DNA fragments were digested with *Xho*I, purified, and then ligated with the pET19b vector (Novagen, Madison, Wis.). The plasmids were introduced into competent *Escherichia coli* JM109 cells and then clones containing the right direction of inserts were selected.

Expression, purification, and refolding of recombinant proteins. *E. coli* BL21 Star(DE3)pLysS cells (Invitrogen, Carlsbad, Calif.) were transformed with the cloned plasmids. Each bacterial clone was cultured in 400 ml of Luria-Bertani (LB) medium containing ampicillin until an optical density at 600 nm (OD_{600}) of 0.6 was achieved. Isopropyl-β-D-thiogalactopyranoside was added to the bacterial cultures to a final concentration of 1 mM, and the cultures were then incubated at 37°C for 3 h. Preparation of inclusion bodies and refolding of the proteins were performed by a using the Protein Refolding Kit (Novagen) essentially according to the manufacturer's recommendations. The bacteria were pelleted by centrifugation and suspended in 16 ml of wash buffer (20 mM Tris-HCl [pH 7.5], 10 mM EDTA, 1% Triton X-100). The suspension was sonicated and then centrifuged. This washing step was repeated five times to obtain the inclusion body. The pellet of the inclusion body was suspended in solubilization buffer (500 mM 3-(cyclohexyamino)-1-propanesulfonic acid (CAPS) [pH 11], 0.3% *N*-lauroylsarcosine) and incubated at room temperature for 15 min. After centrifugation, the supernatant was dialyzed in dialysis buffer (20 mM Tris-HCl [pH 8.5], 0.1 mM dithiothreitol) overnight at 4°C. Dialysis was continued in the buffer without dithiothreitol for 9 h, then in redox refolding buffer (0.2 mM oxidized glutathione, 1 mM reduced glutathione) overnight at 4°C, and finally for 3 h at room temperature.

SDS-PAGE and Western immunoblot analysis. Recombinant proteins were treated with an equal volume of the sample buffer (13) containing 2 mM phenylmethylsulfonyl fluoride, 2 mM TLCK (*Nα-p*-tosyl-L-lysine chloromethyl ketone), 2 mM *p*-hydroxymercuriphenyl sulfonic acid, and 4 μM leupeptin for 5 min at 95°C and then subjected to sodium dodecyl sulfate-polyacrylamide gel electrophoresis (SDS-PAGE). For the Western immunoblot analysis, the protein bands were transferred to polyvinylidene difluoride membranes (26). After a blocking step with 3% skim milk in 10 mM phosphate-buffered saline (PBS; pH 7.4), each strip was incubated with serum samples diluted 1:100 in PBS containing skim milk for 1 h. After being washed with PBS containing 0.05% Tween 20 (PBS-Tween), the strips were treated with horseradish peroxidase (HRP)-conjugated goat antibody to human immunoglobulin G (IgG; whole molecule; ICN Pharmaceuticals, Aurora, Ohio). Development was by the Konica Immunostaining HRP-1000 kit (Konica Co., Tokyo, Japan).

Serum samples. A total of 162 serum samples were studied. Sera from 23 patients with an amebic liver abscess and sera from 34 patients with amebic colitis but without a liver abscess were used as symptomatic cases. The diagnosis of these patients was based on their clinical symptoms, positive serology in an indirect immunofluorescent antibody test, ultrasound examination (liver abscess), endoscopic or microscopic examination (colitis), and prompt response to treatment with metronidazole except for a liver abscess patient who died. Sera from 15 asymptomatic cyst passers, obtained from children in institutions for the mentally retarded, were also studied. In these asymptomatic cyst passers, cysts were identified as *E. histolytica* but not *E. dispar* by PCR (17, 25). In addition, sera from 40 individuals with infection of other protozoa, *Blastocystis hominis* infection (23 cases), malaria (7 cases), toxoplasmosis (7 cases), and giardiasis (3 cases), were used. Most of the serum samples except for asymptomatic cyst passers were obtained from hospitalized patients and outpatients in Tokai University Hospital, Tokyo Metropolitan Komagome Hospital, and St. Luke's International Hospital in Tokyo. As a negative control, sera obtained from 50 healthy individuals with no known history of amebiasis and no parasites in their stools were also used. All of the serum samples were stored at −30°C or at −80°C before use.

ELISA. Crude antigen was prepared from trophozoites of *E. histolytica* HM-1: IMSS axenically grown in BI-S-33 medium (9). After 3 washes with ice-cold PBS, trophozoites were sonicated and centrifuged at 12,000 × *g* for 30 min. The supernatant was used as crude antigen. Enzyme-linked immunosorbent assay (ELISA) was performed in duplicate on serum samples in 96-well flat-bottom microtiter plates (Coaster, Corning, N.Y.). The wells of the ELISA plates, containing 1 μg of crude antigen or 100 ng of recombinant Igl antigens diluted with 50 mM sodium bicarbonate buffer (pH 9.6), were incubated overnight at 4°C. The plates were washed with PBS-Tween and then treated with PBS containing 1% skim milk for 1 h. A total of 100 μl of the serum samples diluted 1:400 with PBS were added to the wells, followed by incubation for 1 h at room temperature. After being washed, the wells were incubated with 100 μl of HRP-conjugated goat antibody to human IgG (whole molecule; ICN Pharmaceuticals) for 1 h at room temperature. After being washed with PBS-Tween, the wells were incubated with 200 μl of substrate solution (0.4 mg per ml of *o*-phenylenediamine in citric acid-phosphate buffer [pH 5.0] containing 0.001% hydrogen peroxide). After 30 min of incubation, the reaction was stopped by the addition of 50 μl of 2.5 M H_2SO_4, and the OD_{490} was recorded by using a Bio-Rad (Hercules, Calif.) model 550 microplate reader. The cutoff point for a positive result was defined as an ELISA value with >3 standard deviations above the mean of the healthy negative controls. OD values were plotted and analyzed by using computer graphics software Prism version 4.0 (GraphPad, San Diego, Calif.).

RESULTS

Expression of recombinant fragments of *E. histolytica* Igl. Igl constructs prepared in the present study were full-length Igl and three partial fragments of Igl: F-Igl (aa 14 to 1088), N-Igl (aa 14 to 382), M-Igl (aa 294 to 753), and C-Igl (aa 603 to 1088). In the design of the constructs, N-Igl and M-Igl, as well as M-Igl and C-Igl, shared overlapping regions to reduce the possible loss of antigenic epitopes in the recombinant fragments. In addition, the region where CXXC motifs were not found in Igl, aa 399 to 524, were included in only M-Igl. All of the four recombinant proteins were expressed in bacteria as inclusion bodies. The purity of the refolded proteins was analyzed by SDS-PAGE (Fig. 1). The apparent molecular masses of these proteins in 7.5% gel were 150 kDa for F-Igl, 53 kDa for N-Igl, 67 kDa for M-Igl, and 85 kDa for C-Igl. Since minor protein bands still existed in F-Igl, Western immunoblot analysis was performed to confirm the antigenicity of the recombinant protein (Fig. 2). Serum samples from four individuals each from among cases of amebic liver abscess, amebic colitis, and asymptomatic cyst passers were used in the analysis. All of these sera were reactive with the 150-kDa F-Igl band. On the other hand, two sera from patients with giardiasis did not react with the band of F-Igl as well as a serum from the healthy control.

ELISA reactivity of recombinant fragments with sera from patients with amebiasis. The reactivities of four recombinant proteins—F-Igl, N-Igl, M-Igl, and C-Igl—with patients' sera were examined by ELISA and compared to that of crude antigen (Fig. 3). When crude antigen was used in the ELISA, all of the sera from individuals with *E. histolytica* infection were scored as positive (sensitivity, 100%), and 5 of 90 negative control sera were judged as positive (specificity, 94%). By the use of F-Igl as the ELISA antigen, all of the sera from asymptomatic cyst passers were positive, but 2 of 23 sera from pa-

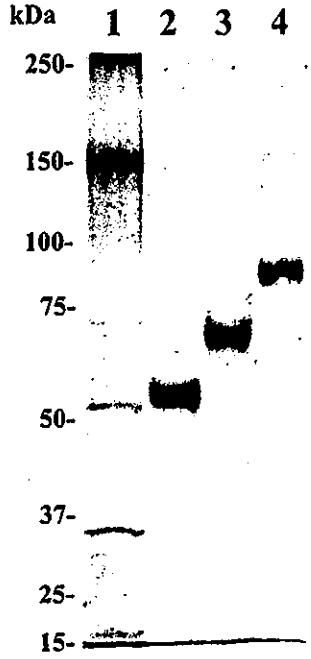

FIG. 1. SDS-PAGE analyses of recombinant Igl. A total of 4 μg of refolded proteins was electrophoresed in a 7.5% gel under reducing conditions. Protein bands were visualized with Coomassie brilliant blue. Lane 1, F-Igl; lane 2, N-Igl; lane 3, M-Igl; lane 4, C-Igl. The numbers to the left indicate molecular masses of size markers.

tients with liver abscess and 5 of 34 sera from patients with colitis were scored as negative (sensitivity, 90%). In the negative controls, five of 90 (four of *B. hominis* infections and one of the healthy controls) results were false positives (specificity, 94%). When three fragments were used as antigens, the mean OD values in the sera from patients with amebiasis were as follows: C-Igl > M-Igl > N-Igl. In the ELISA with N-Igl, sera from 9 cyst passers, sera from 6 patients with liver abscess, and sera from 17 patients with colitis were judged to be negative (sensitivity, 56%). Three sera from patients with malaria and a serum from *B. hominis*-infected individuals were positive (specificity, 96%). When M-Igl was used as an antigen, all of the cyst passers and patients with liver abscess were scored as seropositive, but six of the patients with colitis were seronegative (sensitivity, 92%). In the controls, only one of the *B. hominis*-infected individuals was seropositive (specificity, 99%). With the use of C-Igl, there were two false-negative cases, both of which were patients with colitis (sensitivity, 97%), whereas there was only one false-positive case, which was from a patient with malaria (specificity, 99%). OD values obtained with the ELISA using C-Igl were compared to those obtained with the crude antigen-based ELISA (Fig. 4). There was a significant correlation between the results of these two ELISA tests ($r = 0.8115$; $P < 0.0001$).

DISCUSSION

The results of the present study demonstrate that recombinant Igl is recognized well not only by sera from symptomatic patients with amebic liver abscess and amebic colitis but also by sera from asymptomatic patients in both Western immunoblotting and ELISA. This observation is coincident with the previous data in which affinity-purified native protein was recognized by sera from symptomatic and asymptomatic individuals in a Western immunoblot analysis (8).

In the ELISA system reported in the present study, only 100 ng of antigen was used for the coating of each well of the microplates. The OD values in this concentration were almost comparable with those in 1 μg of crude antigen. This fact demonstrates that the recombinant Igls possess high antigenicity. To date, several recombinant proteins of *E. histolytica* were prepared, and their efficacy in serodiagnosis was examined. When recombinant fragments derived from Hgl were used, sensitivities were 90 to 95% (18, 19, 28). With the use of other antigens, sensitivities were 100% for a 125-kDa surface antigen (14), 88% for 43.5-kDa alcohol dehydrogenase (12), and 82% for serine-rich 46- to 52-kDa antigens (SREHP) (22). In contrast, when a cysteine-rich 29-kDa surface antigen was used, sensitivity of the sera from patients with liver abscess was 76% but only 8% in samples from patients with colitis (20). In comparison with these previous reports, the sensitivity of C-Igl demonstrated in the present study (99%) was considerably higher. Although it is not clear at present how Hgl and Igl associate as a surface lectin complex, the present study demonstrated that Igl, as well as Hgl, is a valuable molecule for diagnostic purposes.

The most interesting observations in the present study were the different reactivities of three Igl fragments with sera from individuals with *E. histolytica* infections. Although high sensi-

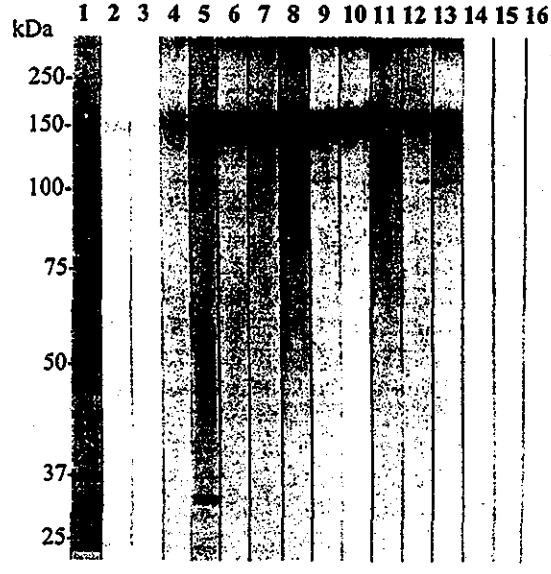

FIG. 2. Western immunoblot analysis of human sera reactivity with F-Igl. Purified F-Igl was subjected to SDS-PAGE in a 7.5% gel under reducing conditions and then transferred to polyvinylidene difluoride membranes. Protein bands of lane 1 were stained with Coomassie brilliant blue. Lanes 2 to 5, sera from individuals who were asymptomatic *E. histolytica* cyst passers; lanes 6 to 9, sera from patients with amebic colitis; lanes 10 to 13, sera from patients with amebic liver abscess; lanes 14 and 15, sera from patients with giardiasis; lane 16, serum from healthy controls. Sera were analyzed following the addition of HRP-conjugated goat antibody to human IgG (whole molecule) as the second antibody. The numbers to the left indicate molecular masses of size markers.